Table 1 – Results of the first neurological evaluation.

Neurological evaluation	Enrich	Standard	Control
Neurological Severity Score	8.5±1.4	8.0±1.1	0.2±0.4*,**
Inclined plane test (angle)			
Head-up	40.0±4.8	42.2±3.1	48.4±2.9*,**
Head-right	36.4±7.0	42.4±2.8	49.9±2.8*,**
			(mean±SD)

Enrich indicates enriched environment group; ST, standard group.
* $p<0.05$ vs. Enrich
** $p<0.05$ vs. ST

have no neurological deficits before transient MCA occlusion (t-MCAO). Evaluation of NSS was examined 72–96 h after t-MCAO at the first evaluation. To compare rats of almost equal neuronal damage, only the rats that scored 7–12 at the first evaluation were used for the subsequent examinations (Table 1). After the first evaluation, rats were housed in an enriched environment (enriched group; $n=10$) or standard cages (standard group; $n=8$). The normal control group (control group; $n=10$) was housed in standard cages. The second evaluation was done at day 14 and the third was done at day 28 after divided into groups. The enriched group was housed in larger cages (610×460×460 mm), and 4–6 rats were housed together. The enriched cage contained various toys, for example, a running wheel, tunnel, etc., and the location of objects in cage including toys, food, and water were rearranged twice a week. The size of the standard cage was 320×210×130 mm, and the standard and control groups were separately housed in each cage. All groups were housed under a 12-h light/dark cycle.

To evaluate the motor deficits, we performed the inclined plane test at the same time of measuring NSS. All rats were confirmed not to have any motor deficits before t-MCAO. Each rat was initially placed on a stainless steel plane inclined at a 30° angle. The angle of the inclined plane was then increased at a rate of 2°/s, and we measured the angle at which the rat's limbs slipped. The inclined plane test was performed with the head in two different orientations: head-up and head-right. For the presentation of the NSS and inclined plane test results, we calculated the mean value of the recovery ratio of the condition at 2 and 4 weeks after t-MCAO to that of the first evaluation for each group. There were no significant differences of neurological function between the enriched environment and standard groups in the first evaluation (Table 1).

5.3. *Brain preparation and histological examinations*

Four weeks after the rats were divided into the three groups, brain tissues were perfused with cold saline, and the animals were sacrificed by exsanguination under chloral hydrate anesthesia. Brains were then cut into 3 coronal sections at 3 mm intervals from the frontal pole. The first blocks (peri-infarct area) and the third blocks (peri-infarct and infarct core areas) were frozen in isopentane–dry ice and stored at −80 °C for gene analysis, and the second blocks (peri-infarct and infarct core areas) were embedded in paraffin for histological analysis. We used the first and second blocks in the present study.

The second blocks were stained by immunohistochemistry using an anti-microtubule-associated protein 2 (MAP-2), a neuronal skeletal protein, antibody. Deparaffinized cortical sections (5 μm) were preincubated with 10% normal pig serum (Kohjin Bio Co., Ltd.). The sections were incubated with the monoclonal anti-MAP-2 antibody (1:400; Pharmingen) overnight at 4 °C. The following day, the sections were rinsed and incubated with biotin-conjugated pig IgG (1:500; Dako) and peroxidase-conjugated streptavidin (1:500; Dako) for 30 min and visualized with diaminobenzidine (DAB) and counterstained with hematoxylin. Immunoreactivities to MAP-2 were measured using VHX-100 (KEYENCE). The infarct area was calculated as follows: infarct area (%) = (MAP-2 staining area in intact side − MAP-2 staining area in ischemic side)/MAP-2 staining area in the intact side × 100.

5.4. *Gene analysis*

cDNA array analysis was conducted using the Rat Genome 230.2.0 Array and GeneChip Instrument System (Affymetrix) containing approximately 28,000 genes. Poly(A)$^+$-RNA extracted from the first blocks in the ischemic side from the enriched group ($n=3$) were pooled and those from 3 animals in the standard group were also pooled. The normalized gene expression signals were compared between the 2 groups. We performed cDNA array analysis for 2 times in this study. For cDNA array analysis, we selected those genes with increases in their normalized gene expression signals above 1.1-fold or decreases below 0.9-fold both 2 times and whose function was known.

5.5. *Real-time quantitative reverse transcriptase–polymerase chain reaction (real-time RT–PCR)*

Real-time quantitative reverse transcriptase–polymerase chain reaction (real-time RT–PCR) was used to confirm the changes in gene expression identified using cDNA array analysis. Eighteen samples were obtained from the bilateral cortices of the first blocks in nine animals (enriched group, $n=3$; standard group, $n=3$; and normal group, $n=3$). Total RNA from the samples was isolated using the acid guanidinium thiocyanate procedure and analyzed for the expression of the 4 identified genes (BDNF, nectin-3, Egr-1, and -2) using real-time RT–PCR (Mx3005; Stratagene). After converting total RNA (5 μg) to cDNA using SuperScript III reverse

Table 2 – Oligonucleotide primers used in real-time quantitative RT–PCR.

Gene	Sequences (forward primer) (Reverse primer)
Nectin 3	TGGTTTATTGGCGTCAGACA (f958)
	GATCCTGGACGTCAGCAGTT (r1119)
BDNF	AGGACGCGGACTTGTACACT (f930)
	GCTGTGACCCACTCGCTAAT (r1115)
Egr-1	AACAACCCTACGAGCACCTG (f549)
	AGGCCACTGACTAGGCTGAA (r750)
Egr-2	AGCTGCCTGACAGCCTCTAC (f402)
	GTTTCTAGGCGCAGAGATGG (r604)

transcriptase (Invitrogen), quantitative PCR was performed using SYBR Green Realtime PCR Master Mix Plus (Toyobo, Japan). The sequence of the primer pairs for each of the genes and their cycling number (N) are described in Table 2. The cycling conditions were 3 min at 95 °C, followed by 40 cycles of 95 °C for 15 s and 67 °C for 30 s. The expression levels of each mRNA were normalized to those of GAPDH mRNA.

5.6. *Data analysis*

A Student's *t* test was used to analyze differences in the infarct areas between the enriched and standard groups and gene expression between the hemispheres in each group. A Tukey–Kramer test was used to evaluate the recovery ratio of neurological functions. A one-way analysis of variance (ANOVA) followed by Fisher's post-hoc test was used to assess the differences in hemispheric gene expression among the 3 groups. A two-tailed *p*-value of <0.05 was considered to be significant. Data are expressed as the mean ± standard deviation.

Acknowledgments

This study was supported in part by a grant from the Mitsubishi Pharma Research Foundation, by research grants for cardiovascular diseases (21A-4, 22-4-1) from the Ministry of Health, Labor, and Welfare of Japan, and by a grant-in-aid for scientific research from the Japan Society for the Promotion of Science.

Disclosures

None.

REFERENCES

Biernaskie, J., Corbett, D., 2001. Enriched rehabilitative training promotes improved forelimb motor function and enhanced dendritic growth after focal ischemic injury. J Neurosci. 21, 5272–5280.

Chen, J., Li, Y., Wang, L., Zhang, Z., Lu, D., Lu, M., Chopp, M., 2001. Therapeutic benefit of intravenous administration of bone marrow stromal cells after cerebral ischemia in rats. Stroke. 32, 1005–1011.

Cramer, S.C., Nelles, G., Benson, R.R., Kaplan, J.D., Parker, R.A., Kwong, K.K., Kennedy, D.N., Finklestein, S.P., Rosen, B.R., 1997. A functional MRI study of subjects recovered from hemiparetic stroke. Stroke. 28, 2518–2527.

Diamond, M.S., Staunton, D.E., de Fougerolles, A.R., Stacker, S.A., Garcia-Aguilar, J., Hibbs, M.L., Springer, T.A., 1990. ICAM-1 (CD54): a counter-receptor for Mac-1 (CD11b/CD18). J Cell Biol. 111, 3129–3139.

Keyvani, K., Sachser, N., Witte, O.W., Paulus, W., 2004. Gene expression profiling in the intact and injured brain following environmental enrichment. J Neuropathol Exp Neurol. 63, 598–609.

Kim, M.W., Bang, M.S., Han, T.R., Ko, Y.J., Yoon, B.W., Kim, J.H., Kang, L.M., Lee, K.M., Kim, M.H., 2005. Exercise increased BDNF and trkB in the contralateral hemisphere of the ischemic rat brain. Brain Res. 1052, 16–21.

Kim, W.S., Kim, I.S., Kim, S.J., Wei, P., Hyung Choi, D., Han, T.R., 2009. Effect of electroacupuncture on motor recovery in a rat stroke model during the early recovery stage. Brain Res. 1248, 176–183.

Kuge, Y., Minematsu, K., Yamaguchi, T., Miyake, Y., 1995. Nylon monofilament for intraluminal middle cerebral artery occlusion in rats. Stroke. 26, 1655–1657 discussion 1658.

Lawrence, M.B., Smith, C.W., Eskin, S.G., McIntire, L.V., 1990. Effect of venous shear stress on CD18-mediated neutrophil adhesion to cultured endothelium. Blood. 75, 227–237.

Moraska, A., Deak, T., Spencer, R.L., Roth, D., Fleshner, M., 2000. Treadmill running produces both positive and negative physiological adaptations in Sprague–Dawley rats. Am J Physiol Regul Integr Comp Physiol. 279, R1321–R1329.

Muller, H.D., Hanumanthiah, K.M., Diederich, K., Schwab, S., Schabitz, W.R., Sommer, C., 2008. Brain-derived neurotrophic factor but not forced arm use improves long-term outcome after photothrombotic stroke and transiently upregulates binding densities of excitatory glutamate receptors in the rat brain. Stroke. 39, 1012–1021.

Nygren, J., Wieloch, T., 2005. Enriched environment enhances recovery of motor function after focal ischemia in mice, and downregulates the transcription factor NGFI-A. J Cereb Blood Flow Metab. 25, 1625–1633.

Ohlsson, A.L., Johansson, B.B., 1995. Environment influences functional outcome of cerebral infarction in rats. Stroke. 26, 644–649.

Okada, Y., Copeland, B.R., Mori, E., Tung, M.M., Thomas, W.S., del Zoppo, G.J., 1994. P-selectin and intercellular adhesion molecule-1 expression after focal brain ischemia and reperfusion. Stroke. 25, 202–211.

Ploughman, M., Granter-Button, S., Chernenko, G., Tucker, B.A., Mearow, K.M., Corbett, D., 2005. Endurance exercise regimens induce differential effects on brain-derived neurotrophic factor, synapsin-I and insulin-like growth factor I after focal ischemia. Neuroscience. 136, 991–1001.

Ploughman, M., Granter-Button, S., Chernenko, G., Attwood, Z., Tucker, B.A., Mearow, K.M., Corbett, D., 2007. Exercise intensity influences the temporal profile of growth factors involved in neuronal plasticity following focal ischemia. Brain Res. 1150, 207–216.

Ronnback, A., Dahlqvist, P., Svensson, P.A., Jernas, M., Carlsson, B., Carlsson, L.M., Olsson, T., 2005. Gene expression profiling of the rat hippocampus one month after focal cerebral ischemia followed by enriched environment. Neurosci Lett. 385, 173–178.

Taub, E., Uswatte, G., Elbert, T., 2002. New treatments in neurorehabilitation founded on basic research. Nat Rev Neurosci. 3, 228–236.

Tureyen, K., Brooks, N., Bowen, K., Svaren, J., Vemuganti, R., 2008. Transcription factor early growth response-1 induction mediates inflammatory gene expression and brain damage following transient focal ischemia. J Neurochem. 105, 1313–1324.

Weiller, C., Ramsay, S.C., Wise, R.J., Friston, K.J., Frackowiak, R.S., 1993. Individual patterns of functional reorganization in the human cerebral cortex after capsular infarction. Ann Neurol. 33, 181–189.

Yan, S.F., Fujita, T., Lu, J., Okada, K., Shan Zou, Y., Mackman, N., Pinsky, D.J., Stern, D.M., 2000. Egr-1, a master switch coordinating upregulation of divergent gene families underlying ischemic stress. Nat Med. 6, 1355–1361.

Zhao, L.R., Mattsson, B., Johansson, B.B., 2000. Environmental influence on brain-derived neurotrophic factor messenger RNA expression after middle cerebral artery occlusion in spontaneously hypertensive rats. Neuroscience. 97, 177–184.

THE JOURNAL OF BIOLOGICAL CHEMISTRY VOL. 285, NO. 18, pp. 13444–13453, April 30, 2010

Down-regulation of *PROS1* Gene Expression by 17β-Estradiol via Estrogen Receptor α (ERα)-Sp1 Interaction Recruiting Receptor-interacting Protein 140 and the Corepressor-HDAC3 Complex*

Received for publication, September 4, 2009, and in revised form, February 26, 2010 Published, JBC Papers in Press, March 3, 2010, DOI 10.1074/jbc.M109.062430

Atsuo Suzuki[‡], Naomi Sanda[§], Yuhri Miyawaki[‡], Yuta Fujimori[‡], Takayuki Yamada[‡], Akira Takagi[‡¶], Takashi Murate[‡¶], Hidehiko Saito[‖], and Tetsuhito Kojima[‡¶1]

From the [‡]Department of Pathophysiological Laboratory Sciences, Nagoya University Graduate School of Medicine, Nagoya 461-8673, Japan, [§]Department of Clinical Laboratory, Nagoya University Hospital, Nagoya 466-8550, Japan, [¶]Department of Medical Technology, Nagoya University School of Health Sciences, Nagoya 461-8673, Japan, and [‖]Nagoya Central Hospital, Nagoya 453-0801, Japan

Pregnant women show a low level of protein S (PS) in plasma, which is known to be a risk for deep venous thrombosis. 17β-Estradiol (E_2), an estrogen that increases in concentration in the late stages of pregnancy, regulates the expression of various genes via the estrogen receptor (ER). Here, we investigated the molecular mechanisms behind the reduction in PS levels caused by E_2 in HepG2-ERα cells, which stably express ERα, and also the genomic ER signaling pathway, which modulates the ligand-dependent repression of the PSα gene (*PROS1*). We observed that E_2 repressed the production of mRNA and antigen of PS. A luciferase reporter assay revealed that E_2 down-regulated *PROS1* promoter activity and that this E_2-dependent repression disappeared upon the deletion or mutation of two adjacent GC-rich motifs in the promoter. An electrophoretic mobility shift assay and DNA pulldown assay revealed that the GC-rich motifs were associated with Sp1, Sp3, and ERα. In a chromatin immunoprecipitation assay, we found ERα-Sp protein-promoter interaction involved in the E_2-dependent repression of *PROS1* transcription. Furthermore, we demonstrated that E_2 treatment recruited RIP140 and the NCoR-SMRT-HDAC3 complex to the *PROS1* promoter, which hypoacetylated chromatin. Taken together, this suggested that E_2 might repress *PROS1* transcription depending upon ERα-Sp1 recruiting transcriptional repressors in HepG2-ERα cells and, consequently, that high levels of E_2 leading to reduced levels of plasma PS would be a risk for deep venous thrombosis in pregnant women.

Protein S (PS)[2] is a vitamin K-dependent plasma protein that functions as a nonenzymatic cofactor for activated protein C in the down-regulation of the blood coagulation cascade via proteolytic inactivation of coagulant factors Va and VIIIa (1). PS has been also shown to display activated protein C-independent anticoagulant activity in purified systems as well as in plasma (2, 3).

Over the past 2 decades, low levels of plasma PS have become a well established risk factor for the development of deep venous thrombosis (4–6). Hereditary PS deficiency has been shown to be an autosomal dominant trait, and many causative genetic mutations have been described in the PSα gene (*PROS1*) (7). However, PS deficiency can also occur throughout life under acquired conditions such as oral anticoagulant use and liver disease (8). Furthermore, acquired PS deficiency has been reported in individuals with high levels of estrogen during pregnancy and in those taking oral contraception (9–11).

The major source of circulating plasma PS is the hepatocyte (12), but PS is also produced constitutively at low levels by a variety of other cell types throughout the body (13–17). PS circulates in human plasma at a concentration of 0.35 μM in a free form (40%) and a C4b-binding protein-bound form (60%) (18, 19). Two copies of the PS gene located on chromosome 3, the active PSα gene (*PROS1*) and the inactive PSβ pseudogene (*PROS2*), share 96% homology in their coding sequences (20–22). The promoter and first exon are absent from the *PROS2* gene, and the promoter region of *PROS1* has been poorly investigated in contrast to the coding regions. It has been reported that transcription from the *PROS1* promoter is directed from multiple start sites and that the *PROS1* 5′-flanking region lacks the characteristic "CAAT" and "TATA" boxes (23).

Estrogens are important regulators of mammalian growth and metabolism, accomplishing these functions by controlling the expression of specific genes via estrogen receptors (24). The estrogen receptor (ER) is a member of the steroid/nuclear receptor superfamily of transcription factors and is required for the mediation of 17β-estradiol (E_2)-induced responses in multiple tissues and organs (25). The classical ER mechanism of

* This study was supported by grants-in-aid from the Ministry of Education, Culture, Sports, Science, and Technology (19590553), the Ministry of Health and Welfare (Health Sciences Research Grant, Research on Specific Disease), and the Kitamura Memorial Foundation, Japan.

[1] To whom correspondence should be addressed: Nagoya University School of Health Sciences, 1-1-20, Daiko-Minami, Higashi-ku, Nagoya 461-8673, Japan. Tel. and Fax: 81-52-719-3153; E-mail: kojima@met.nagoya-u.ac.jp.

[2] The abbreviations used are: PS, protein S; ChIP, chromatin immunoprecipitation; CS-FBS, charcoal-stripped FBS; DMEM, Dulbecco's modified Eagle's medium; EMSA, electrophoretic mobility shift assay; E_2, 17β-estradiol; ER, estrogen receptor; ERE, estrogen-responsive element; FBS, fetal bovine serum; HDAC, histone deacetylase; LCoR, ligand-dependent corepressor; NCoR, nuclear receptor corepressor; re-IP, re-immunoprecipitation; RIP140, receptor-interacting protein 140; RT, reverse transcription; siRNA, small interfering RNA; iNS, nonspecific siRNA; SMRT, silencing mediator of retinoid and thyroid hormone receptors; Sp, specificity protein; TSA, trichostatin A; WT, wild type.

action involves ligand-induced formation of an ER homodimer that interacts with estrogen-responsive elements (EREs) in target gene promoters and recruits cofactors necessary for transactivation (25). There is increasing evidence that the formation of a classical genomic ER-ERE complex is only one of several genomic and non-genomic pathways of estrogen actions (26–28). Genomic ER associates with other transcription factors such as the activating protein-1 (AP-1) complex, nuclear factor κB (NFκB), and specificity proteins (Sp) to modulate ligand-dependent gene expression (26, 27, 29). In this study, we investigated the molecular mechanisms of the reduction in PS production caused by E_2 as well as the genomic ER signaling pathway that modulates ligand-dependent *PROS1* gene repression in HepG2-ERα cells stably expressing human ERα.

EXPERIMENTAL PROCEDURES

Cell Culture and Reagents—Human hepatoma cell line HepG2 and human breast cancer cell line MCF7 were purchased from American Type Culture Collection (ATCC, Manassas, VA). The cells were cultured in Dulbecco's modified Eagle's medium (DMEM; Wako, Tokyo) supplemented with 5 or 10% fetal bovine serum (FBS; JRH Biosciences, Lenexa, KS) and 100× antibiotic-antimycotic mixed stock solution (Nacalai Tesque, Kyoto, Japan). Human normal hepatocytes (hNhep®) were purchased from Lonza (Walkersville, MD) and cultured in collagen I-coated dishes using the HCM™ BulletKit® according to the manufacturer's protocols. For estrogen assays, cells were cultured in phenol red-free DMEM (Invitrogen) supplemented with 10% charcoal-stripped FBS (CS-FBS) for 3 days. Next day, the cells were cultured in phenol red-free DMEM supplemented with 1% CS-FBS and treated with ethanol (vehicle) or 100 nM E_2 for 48 h. E_2 and trichostatin A (TSA) were purchased from Sigma-Aldrich, and ICI 182,780 was from Tocris Bioscience (Ellisville, MO).

Luciferase Constructs of PROS1 Promoter—First, we isolated a 14-kb BamHI fragment containing the *PROS1* promoter from a human genomic library (Clontech, Mountain View, CA). We used a PCR-amplified DNA probe (−582 to +173 with A of the ATG translation initiation codon as +1), which is the 5′-flanking region of human *PROS1* including a part of exon 1, preventing *PROS2* detection. The library was screened with a DIG-High Prime DNA labeling and detection kit (Roche Applied Science) according to the manufacturer's directions. An XbaI/SalI fragment (−4229 to +117) from the isolated *PROS1* gene was subcloned into pBluescript II KS+ (Stratagene, La Jolla, CA) and removed from −3 to +117 by BstBI/SalI digestion and self-ligation. Subsequently, the *PROS1* −4229/−4 fragment was cloned into a pGL3 Basic-derived vector (gift from Dr. Kokame (30)) (pPROS1/−4229). A series of deletion constructs (pPROS1/−1826, pPROS1/−1119, pPROS1/−582, pPROS1/−338, pPROS1/−236, and pPROS1/−175) were obtained by digestion with the respective restriction enzymes and self-ligation or by PCR amplification. Mutated constructs (pPROS1/−175Mut1, pPROS1/−175Mut2, and pPROS1/−175Mut3) were prepared by mismatch PCR as described elsewhere (31) using the following forward primers (mutated bases are underlined): 5′-CCGAGCTCTTACGCGTGGGAGCGAACGGTCTCCTC-3′ (Mut1), 5′-CCGAGCTCTTACGCGTGGGAGCGGGCGGTCTCCTCCGAACCCGGC-3′ (Mut2), and 5′-CCGAGCTCTTACGCGTGGGAGCGAACGGTCTCCTCCGAACCCGGC-3′ (Mut3). pPROS1/−4229Mut was constructed from pPROS1/−4229 by the QuikChange Lightning site-directed mutagenesis kit (Stratagene) according to the manufacture's instructions using the following primers: 5′-GGAGCGAACGGTCTCCTCCGAACCCGGCTG-3′ and 5′-GCCGGGTTCGGAGGAGACCGTTCGCTCCCA-3′.

ERα Expression Plasmid and Stable Transfectants—Human ERα cDNA was obtained by reverse transcription (RT)-PCR from MCF7 mRNA. We amplified the cDNA as two fragments using as primers 5′-GGGAATTCTTTCTGAGCCTTCTGCCCTG-3′/5′-CATGTCGAAGATCTCCACCATG-3′ for upstream fragments (1347 bp) and 5′-ACCGAAGAGGAGGGAGAATGT-3′/5′-GGCTCGAGCTTGGAATCCCTTTGGCTGT-3′ for downstream fragments (1232 bp). The upstream and downstream PCR products were digested with EcoRI/HindIII and HindIII/XhoI, respectively, and ligated as a full-length human ERα cDNA into the pcDNA3.1 vector (Invitrogen) (pERα).

pERα was transfected by a calcium precipitation method as described previously (32), and stable transfectants were established from HepG2 cells through selection with G418. All clones were checked by Western blot analysis as described below, and the subclone showing the highest level of ERα (HepG2-ERα) was used for further study.

Enzyme-linked Immunosorbent Assay for Measurement of PS—HepG2-ERα cells were treated with E_2 or vehicle (ethanol only) for 48 h, and the culture medium was harvested. A rabbit IgG against human PS (Dako, Carpinteria, CA) was biotinylated with an ECL™ protein biotinylation module (Amersham Biosciences). An unlabeled anti-PS polyclonal antibody (2.4 ng/100 μl) in bicarbonate buffer (15 mM Na_2CO_3, 35 mM $NaHCO_3$, and 3 mM NaN_3) was coated onto each well of a microtiter plate (Nunc, Roskilde, Denmark). After three washes with 150 μl of Tris-buffered saline (TBS; 50 mM Tris, pH 7.4, 150 mM NaCl), the wells were blocked with 1% bovine serum albumin in TBS and then incubated with the plasma standards or culture medium samples. After three more washes with TBS, the biotinylated anti-PS antibody (0.1 μg/100 μl) was added followed by diluted (1:1000) streptavidin-horseradish peroxidase conjugate (Amersham Biosciences). After incubation, the substrate buffer (0.65 mg/ml *o*-phenylenediamine (Wako) and 0.06% H_2O_2 in 0.1 M citrate, 0.2 M sodium phosphate buffer, pH 5.0) was added to each well. After further incubation at room temperature for 20 min, the peroxidase reaction was stopped by the addition of 50 μl of 2 M H_2SO_4, and absorbance was measured at 490 nm.

Quantitative RT-PCR for Measurement of PS mRNA—Total RNA of the cells was extracted using an RNeasy mini kit (Qiagen, GmbH, Germany). The first-strand cDNA was prepared with 5 μg of total RNA using the SuperScript III first strand system (Invitrogen). Quantitative RT-PCR was performed with a Power SYBR Green PCR Master Mix (Applied Biosystems, Foster City, CA), and ABI PRISM 7000 sequence detection systems (Applied Biosystems) were used for measurement. Relative PS mRNA was calculated as the respective PS

mRNA/GAPDH (glyceraldehyde-3-phosphate dehydrogenase) mRNA as described previously (33).

Western Blot Analysis—Proteins were extracted from the cultured cells by harvesting in SDS sample buffer (50 mM Tris-HCl, pH 6.8, 2% SDS, 850 mM 2-mercaptoethanol, 5% glycerol, and 0.001% bromphenol blue). Samples were resolved by 10% SDS-PAGE and transferred to Immonilon-P membranes (Millipore, Bedford, MA). Membranes were blocked with excess protein (2% skim milk) and probed with primary antibody (1:1000) against ERα, Sp1, Sp3 (Santa Cruz Biotechnology, Santa Cruz, CA), or β-actin (Cytoskeleton Inc., Denver, CO). After being washed with phosphate-buffered saline containing 0.05% Tween 20, membranes were probed with a horseradish peroxidase-conjugated secondary antibody (1:1000; Cell Signaling Technology, Danvers, MA) for 1 h. Signals were visualized with a chemiluminescent substrate (ECL Plus Western blotting detection system, Amersham Biosciences).

Luciferase Reporter Assay—Cells were seeded in 35-mm dishes at a concentration of 1.0×10^5 cells in phenol red-free DMEM supplemented with 10% CS-FBS. After 18 h, the appropriate *PROS1* luciferase reporter plasmids (3 μg) and pSV-β-galactosidase plasmid (0.2 μg; Promega, Madison, WI) were transiently co-transfected using Lipofectin® reagent (Invitrogen) according to the manufacturer's protocol.

After a 6-h transfection, the cells were washed and treated for 48 h with fresh phenol red-free DMEM supplemented with 1% CS-FBS containing 100 nM E_2, 100 nM E_2/1 mM ICI 182,780, 1 mM ICI 182,780 only dissolved in ethanol, or ethanol alone as a vehicle control. The cells were harvested, and subsequently luciferase activity was determined with a luciferase assay system (Promega) according to the manufacturer's directions. Luciferase activity was normalized to the activity of co-transfected β-galactosidase as an internal control for transfection efficiency.

Transient Transfection of siRNA—HepG2-ERα cells were cultured in phenol red-free DMEM with 10% CS-FBS and transfected with siRNA against Sp1 or Sp3 (Ambion, Austin, TX) or nonspecific siRNA using Oligofectamine reagent (Invitrogen) according to the manufacturer's directions.

Electrophoretic Mobility Shift Assay (EMSA)—Nuclear extracts were prepared from HepG2-ERα cells using NE-PER® nuclear and cytoplasmic extraction reagents (Pierce) and stored in aliquots at −80 °C until further use. The protein concentration of the nuclear extracts was measured with the Bio-Rad protein assay kit (Bio-Rad). DNA probes containing the *PROS1* promoter fragment (from −176 to −147) were synthesized, biotinylated, and annealed. EMSA was performed according to a method described previously (32). Briefly, nuclear extract (5 μg) and a biotin-labeled double-stranded DNA probe (600 fmol), with or without an unlabeled competitor, were treated with a LightShift™ chemiluminescent EMSA kit (Pierce) according to the manufacturer's instructions. In supershift experiments, the nuclear extract was incubated on ice for 10 min with the biotin-labeled double-stranded DNA probe after which an anti-Sp1, anti-Sp3, or anti-ERα antibody was added, and the incubation was continued for another 20 min. Samples were loaded on a 6% nondenaturing polyacrylamide gel in 0.5× TBE buffer (0.089 M Tris borate, pH 8.0, 0.089 M boric acid, and 10 mM EDTA) and electrophoresed for 3.5 h at 100 V. Biotin-labeled DNA probes were transferred to Hybond™-N+ membranes (Amersham Biosciences) and then integrated with streptoavidin-horseradish peroxidase conjugate.

DNA Pulldown Assay—The DNA pulldown assay (DNA affinity precipitation; DNAP assay) was carried out with biotin-labeled DNA probes as described previously (34). The nuclear extracts (100 μg) were prepared from HepG2-ERα cells and incubated with biotin-labeled DNA probes (100 pmol) and 15 μg of polydI-dC in DNAP buffer (20 mM HEPES-KOH, pH 7.9, 80 mM KCl, 1 mM $MgCl_2$, 0.2 mM EDTA, 0.5 mM dithiothreitol, 10% glycerol, and 0.1% Triton X-100) on ice for 45 min. Subsequently, 500 μg of Dynabeads® M-280 streptavidin (Invitrogen) was added and incubated further at 4 °C for 1 h. The beads were washed three times with DNAP buffer, and the bound proteins were eluted in SDS sample buffer, separated by 10% SDS-PAGE, and characterized by Western blot analysis with the respective specific antibodies.

Chromatin Immunoprecipitation (ChIP) and ChIP Reimmunoprecipitation (Re-IP) Assays—HepG2-ERα cells were treated with E_2 or vehicle and fixed with 2% formaldehyde. The cross-linking reaction was stopped by the addition of 0.125 M glycine. After two washes with phosphate-buffered saline, the cells were resuspended in a swelling buffer (10 mM Tris-HCl, pH 7.6, 3 mM $CaCl_2$, 0.1% Nonidet P-40, and 1× protease inhibitor mixture (Nakalai Tesque)). After incubation on ice for 10 min, the samples were mixed by vortex, and the nuclei were collected. Isolated nuclei were resuspended in SDS lysis buffer (50 mM Tris-HCl, pH 8.0, 1% SDS, 10 mM EDTA, and 1× protease inhibitor mixture) and sonicated to the desired chromatin length (0.5 kb). After centrifugation, the supernatant was diluted with dilution buffer (16.7 mM Tris-HCl, pH 8.0, 167 mM NaCl, and 1.1% Triton X-100) containing 1× protease inhibitor mixture, divided into aliquots, and precleared by the addition of protein A-agarose or protein G PLUS-agarose (Santa Cruz Biotechnology). In the ChIP assay, the precleared chromatin supernatants were immunoprecipitated with the respective antibodies specific to ERα, Sp1, Sp3, nuclear receptor corepressor (NCoR), silencing mediator of retinoid and thyroid hormone receptors (SMRT), histone deacetylase 1 (HDAC1), HDAC3, HDAC4, HDAC5, receptor-interacting protein 140 (RIP140), ligand-dependent corepressor (LCoR) (Santa Cruz Biotechnology), and AcH4 (Millipore) or nonspecific IgG at 4 °C overnight. The protein-antibody complexes were incubated with protein A-agarose or protein G PLUS-agarose at 4 °C overnight. The beads were washed extensively in the following buffers: low salt wash buffer (50 mM Tris-HCl, pH 8.0, 150 mM NaCl, 1 mM EDTA, 1% Triton X-100, 0.1% SDS, 0.1% sodium deoxycholate, and 1× protease inhibitor mixture); high salt wash buffer (50 mM Tris-HCl, pH 8.0, 500 mM NaCl, 1 mM EDTA, 1% Triton X-100, 0.1% SDS, 0.1% sodium deoxycholate, and 1× protease inhibitor); and TE buffer (10 mM Tris-HCl, pH 8.0, 1 mM EDTA). The immunocomplexes were extracted from the beads with elution buffer (0.1 M $NaOH_3$ and 1% SDS) and reversed by heating at 65 °C overnight. Bound DNA was purified with a High Pure PCR cleanup micro kit (Roche Applied Science) and used as a template for subsequent amplification. The primers were 5′-

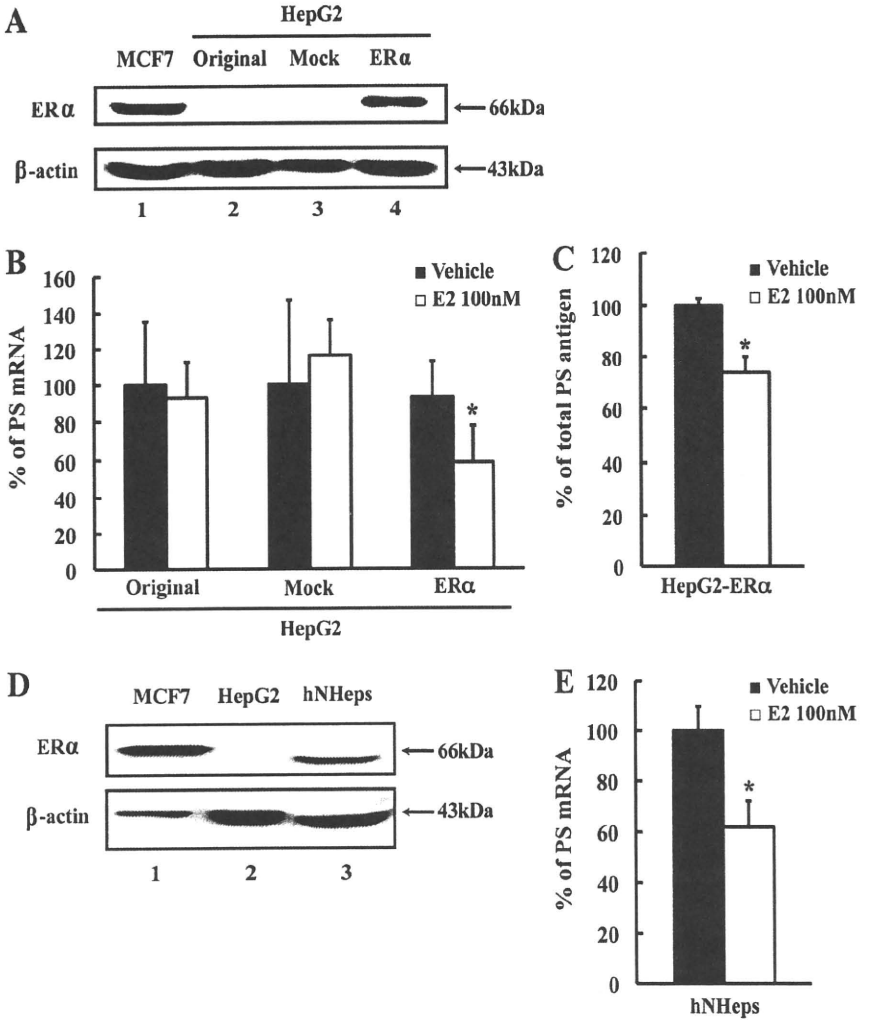

FIGURE 1. **Down-regulation of PS mRNA and antigen in HepG2-ERα cells and human normal hepatocytes by 17β-estradiol.** *A*, analysis of whole cell extract from MCF7 cells used as a positive control (*lane 1*), the original HepG2 cells (*lane 2*), mock-transfected HepG2 cells (*lane 3*), and HepG2-ERα cells (*lane 4*) by Western blotting using anti-ERα antibody. Anti-β-actin antibody was used as a loading control. *B* and *C*, results of quantitative RT-PCR and an enzyme-linked immunosorbent assay to evaluate the effects of E_2 on the levels of PS mRNA in HepG2-ERα cells and its derived cells (*B*) and on the levels of PS antigen secreted from HepG2-ERα cells (*C*). After treatment of HepG2-ERα cells with E_2 for 48 h, total RNA and the culture medium were harvested and analyzed by quantitative RT-PCR and an enzyme-linked immunosorbent assay, respectively. Values are the mean ± S.D. for at least three independent experiments. *, $p < 0.05$ *versus* vehicle control. *D*, analysis of whole cell extract from MCF7 cells used as positive control (*lane 1*), the original HepG2 cells used as negative control (*lane 2*), and hNHep cells (*lane 3*) by Western blotting using anti-ERα antibody. Anti-β-actin antibody was used as a loading control. *E*, results of quantitative RT-PCR to evaluate the effects of E_2 in hNHep.

GCTCCGAAAAGCTTCCTGGAA-3′ (−236/−217, forward) and 5′-CGCCTCGGTCTGAGCCGT-3′ (−88/−105, reverse), which amplified a 149-bp region of the *PROS1* promoter containing target GC-rich motifs. The primers amplifying a 159-bp region of the *PROS1* promoter that contained no GC-rich motif were 5′-GGAGAATGAGGGGCAAGA-3′ (−4033/−4016, forward) and 5′-CATTTCATCACCTTAGCAACCT-3′ (−3875/−3896, reverse), and those amplifying a 175-bp region of the *PROS1* promoter containing a non-target GC-rich motif were 5′-AGGAGAGCAGGGCAGGATAA-3′ (−3748/−3729, forward) and 5′-GGACAGAAGCCCAATCATAGTAAAT-3′ (−3574/−3598, reverse). PCR products were resolved on a 2% agarose gel in the presence of 1 μg/ml ethidium bromide.

In the ChIP re-IP assay, the precleared chromatin supernatants were immunoprecipitated with the first antibody, anti-ERα or anti-RIP140, at 4 °C for overnight. The protein-antibody complexes were incubated with protein G PLUS-agarose at 4 °C for 2–4 h, eluted by incubation with 10 mM dithiothreitol at 37 °C for 30 min, and diluted 1:50 in dilution buffer. After centrifugation, the supernatants were divided in aliquots and reimmunoprecipitated with their respective second antibodies individually. The second immunocomplexes were extracted from the beads followed by PCR amplifications of a 149-bp region of the *PROS1* promoter containing target GC-rich motifs from bound DNA as described above.

Statistical Analysis—Data are presented as the mean ± S.D. and are representative of at least three independent experiments. Significant differences between experimental groups in the quantitative RT-PCR, enzyme-linked immunosorbent assay, and luciferase assay were analyzed using Student's *t* test. Differences were considered to be significant when p was less than 0.05.

RESULTS

Down-regulation of PROS1 Expression by E_2 in HepG2-ERα Cells and Human Normal Heptocytes—Because ERα was undetectable in the original HepG2 cells by Western blotting (Fig. 1*A*), we established a HepG2-derived cell line stably expressing human ERα (HepG2-ERα) as described under "Experimental Procedures." We confirmed that the HepG2-ERα cells expressed large amounts of ERα protein equivalent to breast cancer-derived MCF7 cells as determined by Western blot analysis (Fig. 1*A*). The HepG2-ERα cells treated with E_2 showed significantly decreased levels of PS mRNA, but the original HepG2 cells and HepG2-Mock cells did not (Fig. 1*B*). Also, E_2 treatment down-regulated PS antigen significantly in the HepG2-ERα cells (Fig. 1*C*). In addition, we also demonstrated that E_2 treatment down-regulated PS mRNA by 60% in hNHep, which expressed a high level of ERα protein (Fig. 1, *D* and *E*).

Luciferase Reporter Assay—We next examined *PROS1* promoter activity by conducting a luciferase reporter assay and

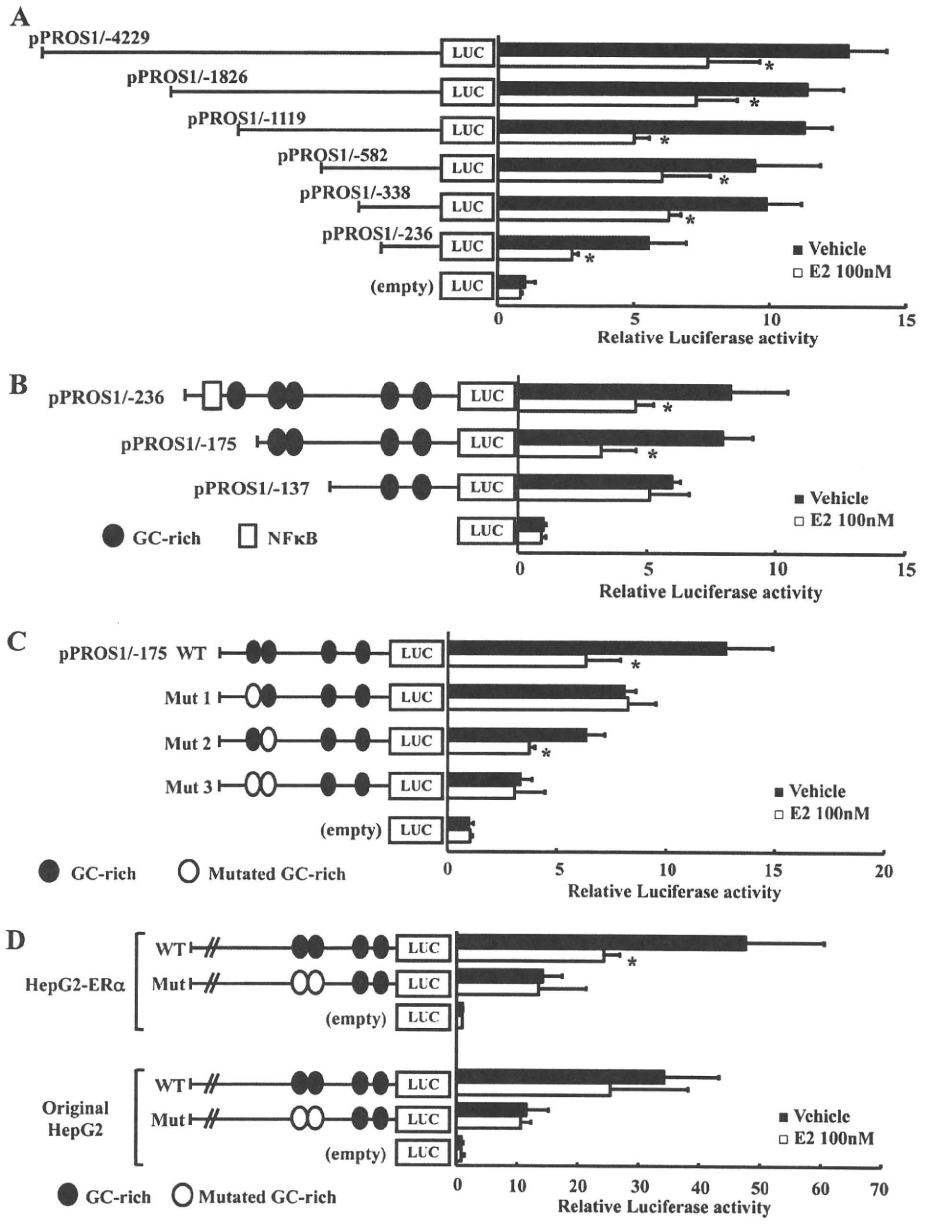

FIGURE 2. **Transient expression of *PROS1* promoter-reporter gene constructs in HepG2-ERα cells with or without E_2 treatment.** Luciferase activity of the HepG2-ERα cells transiently transfected with pPROS1/−4229 or its 5′-deleted constructs (*A* and *B*) and pPROS1/−175 or its mutant (*C*), with or without E_2 treatment, was measured. WT (pPROS1/−4229) or the full-length promoter construct with mutation (pPROS1/−4229Mut) was transiently transfected into HepG2-ERα cells or original HepG2 cells treated with or without E_2, and luciferase activities were measured (*D*). The luciferase activity levels of the respective constructs were expressed as relative values to that of the pGL3 Basic-derived empty vector without E_2 treatment. *A*, results for the constructs pPROS1/−4229 to pPROS1/−236. *B*, results for the constructs pPROS1/−236 to pPROS1/−137 with putative transcription factor binding sites. *C*, analysis of mutations in the GC-rich motifs in pPROS1/−175. Results for constructs pPROS1/−175 WT, Mut1 (−170A/−169A), Mut2 (−156A/−155A), and Mut3 (−170A/−169A/−156A/−155A) are shown. *D*, analysis of mutations in the GC-rich motifs in pPROS1/−4229. Results for WT (pPROS1/−4229) and mutated (pPROS1/−4229Mut) constructs are shown. Values are the mean ± S.D. for at least three independent experiments. *, $p < 0.05$ *versus* vehicle control.

observed that E_2 decreased the luciferase activity of pPROS1/−4229 in HepG2-ERα cells (Fig. 2*A*). In a series of 5′-truncated constructs obtained by restriction enzyme digestion and self-ligation of pPROS1/−4229, we also observed E_2-dependent repression of the luciferase activity, although the basal activity was gradually reduced (Fig. 2*A*). Meanwhile, a computer search for putative nuclear factor binding sites between −338 and −236 revealed AP-1 and GC-rich sites at −281 and −244 that might play a role in the basal expression of *PROS1* in HepG2-ERα cells, respectively.

In a luciferase assay of further truncated forms, pPROS1/−175 showed E_2-dependent repression, but pPROS1/−137 did not, indicating that the −175 to −137 region of the *PROS1* promoter, containing two adjacent GC-rich motifs at −172 to −163 and −162 to −153, was critical for E_2-induced down-regulation (Fig. 2*B*). To clarify the importance of those GC-rich motifs, we transfected a series of constructs containing mutations of a single GC-rich site (pPROS1/−175Mut1 or pPROS1/−175Mut2) or of both sites (pPROS1/−175Mut3). We observed that the luciferase reporter activity of the HepG2-ERα cells transfected with pPROS1/−175Mut2 was reduced by E_2 treatment, but that of the cells transfected with pPROS1/−175Mut1 or pPROS1/−175Mut3 was not (Fig. 2*C*).

To further investigate the importance of the two GC-rich motifs in a full-length promoter, we prepared a luciferase reporter vector with two mutated GC-rich motifs (pPROS1/−4229Mut) derived from pPROS1/−4229. In comparison with pPROS1/−4229, pPROS1/−4229Mut showed a reduced luciferase activity and loss of its E_2-dependent repression in HepG2-ERα cells (Fig. 2*D*). In the original HepG2 cells, which lack ERα expression, pPROS1/−4229 also did not show apparent E_2-dependent repression of the luciferase activity.

Requirement of ERα for E_2-dependent Down-regulation of PROS1 in HepG2 Cells—We also examined the ERα requirement for E_2-induced inhibition of *PROS1* promoter activity in HepG2 cells transfected with pPROS1/−175. The HepG2-ERα cells stably expressing human ERα showed E_2-induced repression of luciferase activity, whereas the HepG2 mock-transfected cells with no ERα expression did not (Fig. 3*A*). Consistent with these observations, ICI 182,780 (a

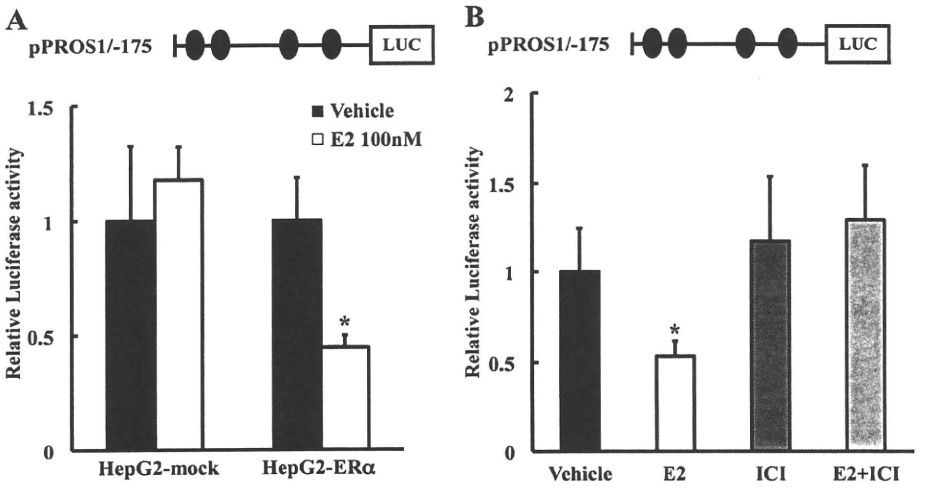

FIGURE 3. **E_2-dependent *PROS1* down-regulation mediated by ERα.** *A*, luciferase (*LUC*) activity levels of cells transfected with pPROS1/−175, with or without E_2 treatment, expressed relative to that of the pGL3 Basic-derived empty vector without E_2 treatment. *B*, HepG2-ERα cells transfected with pPROS1/−175 and treated with 100 nM E_2, 10 μM ICI 182,780, or both. After 48 h, luciferase activities were measured, and results were expressed as relative values to that of the vehicle-treated cells. Values are the mean ± S.D. for at least three independent experiments. *, $p < 0.05$ *versus* vehicle control.

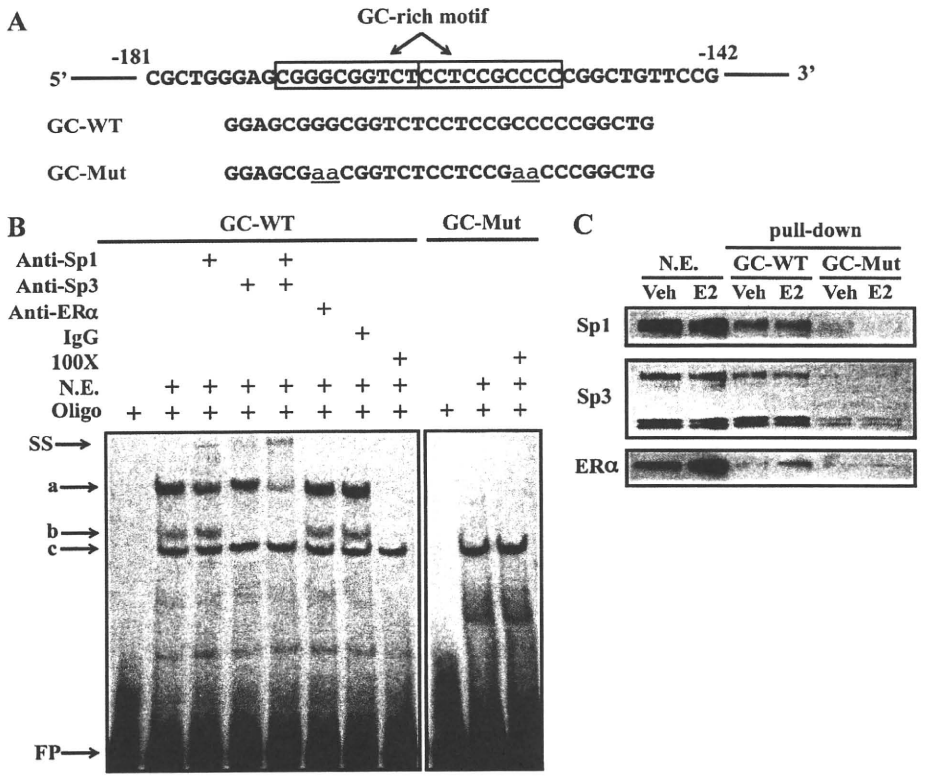

FIGURE 4. **Interaction of Sp and ERα proteins with the *PROS1* promoter *in vitro* and importance of the GC-rich motifs.** *A*, oligonucleotides used in EMSA and DNA pulldown analyses. GC-Mut contains mutations in both the distal and proximal GC-rich motifs. *B*, EMSA was performed with nuclear extracts from HepG2-ERα cells in the presence of the biotin-labeled DNA oligonucleotides GC-WT or GC-Mut. The biotin-labeled oligonucleotides were incubated alone or in combination with 5 μg of nuclear extract (*N.E.*) from E_2-treated HepG2-ERα cells in the presence of a 100-fold molar excess of specific unlabeled oligonucleotide (*100X*) or antibodies. *Arrows* indicate retarded (*a*, *b*, and *c*) and supershifted (*SS*) complexes. *FP*, free probe. *C*, DNA pulldown assays carried out by incubating biotin-labeled oligonucleotides containing WT or mutated GC-rich motifs with nuclear extract from HepG2-ERα cells with or without E_2 treatment. Specifically bound proteins were eluted and subjected to Western blotting using specific antibodies against Sp1, Sp3, and ERα, respectively. Similar results were obtained in multiple independent experiments. *Veh*, vehicle.

pure antagonist of ER) reversed the effects of E_2 on luciferase activity in HepG2-ERα cells transfected with pPROS1/−175, whereas ICI 182,780 alone had no effect (Fig. 3*B*).

Sp1 and Sp3 Bind to GC-rich Motifs of the PROS1 Promoter in Vitro—To identify the transcription factors binding to the GC-rich motifs at −173 and −162 of the *PROS1* promoter in HepG2-ERα cells treated with E_2, EMSAs and DNA pulldown assays were carried out. The oligonucleotides used in the EMSAs and DNA pulldown assays are shown in Fig. 4*A*. In the EMSAs, three shifted bands (*a*–*c*) were detected using wild-type probes (GC-WT), two (*a* and *b*) of which were not detected using mutated oligonucleotides (GC-Mut) that destroyed both GC-rich motifs (Fig. 4*B*). Furthermore, co-incubation with a 100-fold excess of nonlabeled GC-WT oligonucleotides reduced the intensity of each of these two bands, but the third shifted band (*c*) was still present. These results indicate that the first two bands (*a* and *b*) were specific shifted bands, and the third (*c*) was nonspecific. In the supershift experiment, co-incubation with antibody against either Sp1 (*a*) or Sp3 (*b*) gave reduced shifted bands and additional supershifted bands (*SS*). Antibodies against ERα and nonspecific IgG, however, did not affect the intensity of the shifted bands. DNA pulldown assays gave results consistent with the EMSAs, indicating that Sp1 and Sp3 were apparently co-purified with the wild-type oligonucleotides but not with the mutated oligonucleotides (Fig. 4*C*). The Sp proteins were detected in the nuclear extracts regardless of E_2 treatment. In contrast, we detected more ERα signals in the nuclear extracts from E_2-treated cells than in those from untreated cells, probably because of the increase in ERα proteins in the nucleus due to E_2 stimulation.

Knockdown Experiments with siRNA for Sp Proteins—To verify the function of Sp1 and Sp3 in the

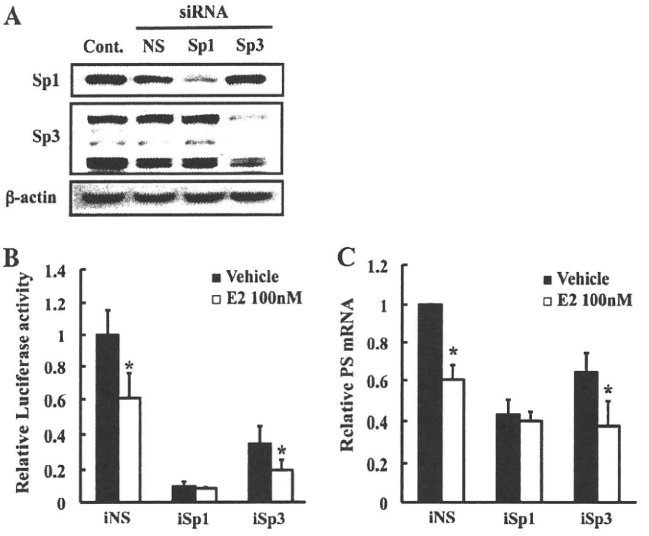

FIGURE 5. **Knockdown of Sp1 or Sp3 by RNA interference and its effects on E_2-dependent *PROS1* repression.** *A*, knockdown of Sp was determined by Western blotting. HepG2-ERα cells were transfected with iNS, iSp1, or iSp3, and whole cell lysate was analyzed by Western blotting as described under "Experimental Procedures." The experiments were repeated at least three times, and similar results were obtained. β-Actin was used as a loading control (*Cont.*). *B*, RNA interference-luciferase reporter analysis of HepG2-ERα cells. siRNAs (50 nM) were transfected, and the next day pPROS1/−175 was transfected with or without E_2 treatment. Luciferase activity was expressed relative to that of the cells without E_2 treatment. *C*, quantitative RT-PCR analysis after siRNA transfection in HepG2-ERα cells. Cells were transfected with respective siRNAs for 4 h and treated with E_2 for 48 h. Values are the mean ± S.D. for at least three independent experiments. *, $p < 0.05$ *versus* vehicle control.

repression of *PROS1* by E_2, we carried out RNA interference experiments. A Western blot analysis of whole lysate from HepG2-ERα cells transfected with nonspecific siRNA (iNS) showed that Sp1 and Sp3 were almost equally expressed compared with levels in untransfected control cells (Fig. 5*A*). However, in the cells transfected with siRNAs for Sp1 (iSp1) and Sp3 (iSp3), a decreased expression of Sp1 and Sp3 proteins was observed, respectively. We next investigated the effects of Sp1 or Sp3 knockdown by conducting luciferase reporter experiments. After the co-transfection of both siRNA and the luciferase reporter construct (pPROS1/−175), HepG2-ERα cells were treated with E_2, and luciferase activity was determined (Fig. 5*B*). Basal luciferase activity was decreased in the cells transfected with iSp1 or iSp3 compared with the cells transfected with iNS. E_2-dependent repression of luciferase activity occurred in the cells transfected with iNS or iSp3 but not in the cells transfected with iSp1. We also observed consistent results for PS mRNA levels in the cells transfected with siRNAs (Fig. 5*C*). These results indicate that Sp1 and Sp3 are important for basal *PROS1* transcription and that Sp1 also has a crucial role in E_2-dependent repression.

ChIP and ChIP Re-IP Assays—The interactions of ERα, Sp proteins, corepressors, and HDACs with the proximal region of the *PROS1* promoter were further investigated in ChIP and ChIP re-IP assays. In the ChIP assay, the chromatin supernatants from HepG2-ERα cells treated with E_2 or vehicle were immunoprecipitated with specific antibodies against nuclear proteins (ERα, Sp1, Sp3, NCoR, SMRT, HDAC1, HDAC3, HDAC4, HDAC5, and AcH4) or nonspecific IgG, and the eluted DNA fragments were used as subsequent PCR templates for amplification of the region containing target GC-rich motifs in the *PROS1* promoter (Fig. 6*A*). We also used 5′-upstream regions containing non-target GC-rich motifs or no GC-rich motif for control PCR amplifications. As shown in Fig. 6*B*, ERα was recruited to the *PROS1* promoter region containing target GC-rich motifs in an E_2-dependent manner, although little was recruited to the control regions. Sp1 was also detected without E_2 treatment, but its expression was clearly enhanced by E_2, whereas Sp3 was recruited in an E_2-independent manner. We further investigated the possible commitment of other corepressors and found that NCoR and SMRT were also recruited to the region containing target GC-rich motifs in an E_2-dependent manner (Fig. 6*B*, *left*).

Because liganded ERα is not known to recruit NCoR-SMRT corepressors directly, we tried ChIP assays for RIP140, which is known to interact with liganded ER and modulate ER-mediated transcription (35), and for LCoR, which is an NR-box-containing factor the same as RIP140 (36). After E_2 treatment, only RIP140 was strongly recruited to the region including target GC-rich motifs but not to the other regions (Fig. 6*B*, *middle*).

In addition, we investigated the recruitment of HDACs, which are known to interact with RIP140 (37), and observed class I HDACs; HDAC3 was expressed robustly, and HDAC1 was expressed slightly after E_2 treatment (Fig. 6*B*, *right*). Class II HDAC4 and HDAC5 were not affected by E_2. Meanwhile, acetylated histone H4 was deacetylated in the region around the *PROS1* promoter containing target GC-rich motifs following E_2 treatment (Fig. 6*B*, *right*).

Furthermore, to confirm the E_2-dependent complex formation of those repressive proteins on the *PROS1* promoter, we tried ChIP re-IP assays. We used anti-ERα or anti-RIP140 for primary immunoprecipitation and antibodies against the respective nuclear factors for secondary immunoprecipitation. As expected, we observed similar results in both of the ChIP re-IP assays using anti-ERα and anti-RIP140 as the primary antibodies, respectively, which showed that ERα, RIP140, Sp1, Sp3, NCoR-SMRT, and HDAC3 were present on the same region of the *PROS1* promoter containing target GC-rich motifs (Fig. 6*C*). Additionally, we observed that the blocking of deacetylation by an HDAC inhibitor, TSA, cancelled the E_2-dependent *PROS1* gene repression (Fig. 6*D*).

DISCUSSION

The action of estrogen in target cells is regulated via estrogen receptors that modulate gene expression either positively or negatively. Recent studies have clarified that E_2-ER functions as a gene modulator, although its negative effects on gene expression are less well understood than its positive effects. We investigated here the molecular mechanisms by which E_2-ER negatively regulates the gene expression of the anticoagulant PS.

First, we established a cell line (HepG2-ERα) stably expressing human ERα, because ERα was undetectable in HepG2 cells, and found that E_2 treatment of HepG2-ERα cells significantly down-regulated PS expression. The luciferase assays suggested that the GC-rich motif at −172 of the *PROS1* promoter plays an important role in E_2-dependent gene repression. In subsequent

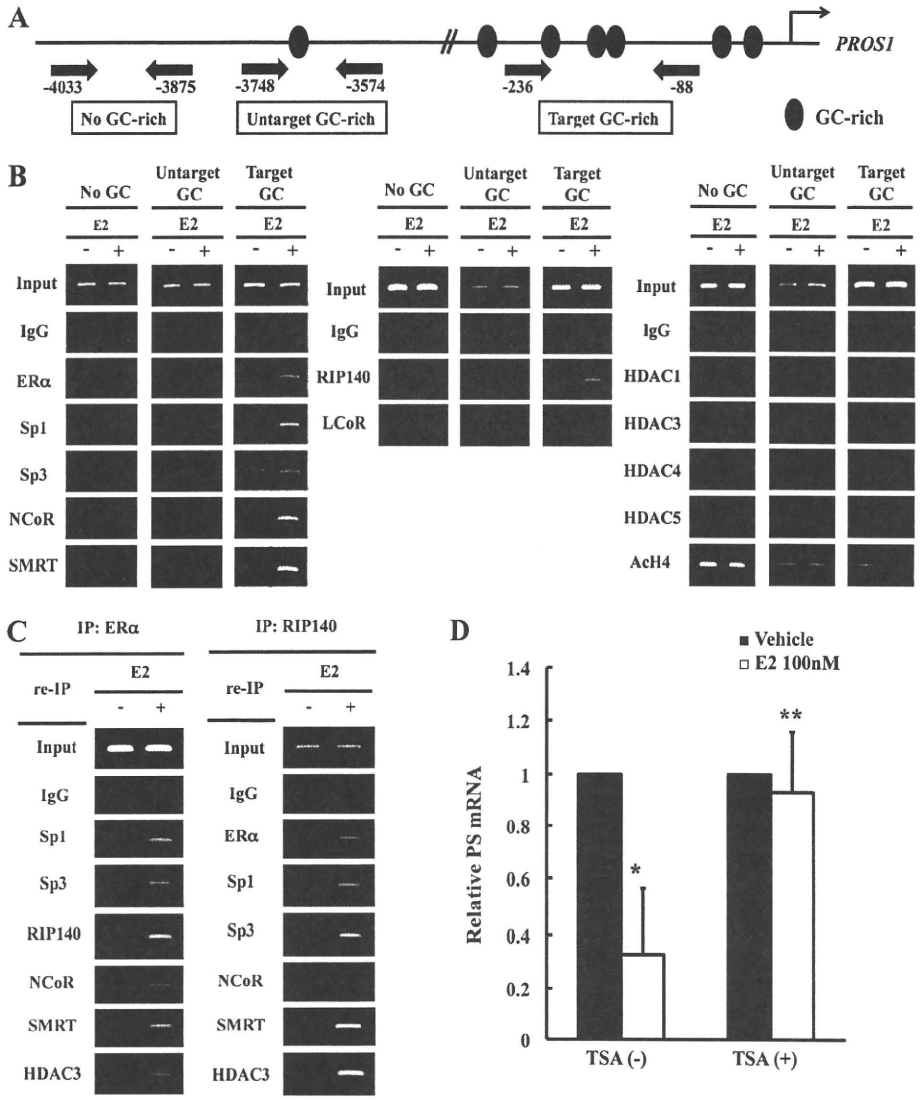

FIGURE 6. **ChIP and ChIP re-IP analyses of the E_2-responsive region or control regions of the *PROS1* promoter and the effect of TSA on E_2-dependent *PROS1* repression.** *A*, ChIP analysis of the E_2-responsive region containing GC-rich motifs in the *PROS1* promoter and of the control regions containing no GC-rich motif a or non-target GC-rich motif. Specific primers for detection of respective regions (*Target GC-rich*, −236 and −88; *Untarget GC-rich*, −3748 and −3574; *No GC-rich*, −4033 and −3875) are represented by *thick arrows*. *B*, ChIP assays for HepG2-ERα cells treated with E_2 or vehicle control performed using various antibodies. Similar results were obtained in multiple independent experiments. *C*, ChIP re-IP assays for HepG2-ERα cells treated with E_2 or vehicle control performed using anti-ERα antibody or anti-RIP140 antibody for primary immunoprecipitation (*IP*). Re-immunoprecipitation was performed with respective antibodies as described. *D*, HepG2-ERα cells were treated with E_2, TSA, or the two in combination, and total RNA was harvested and analyzed by quantitative RT-PCR. Values are the mean ± S.D. for at least three independent experiments. *, $p < 0.05$ *versus* vehicle control; **, $p < 0.05$ *versus* TSA(−) + E_2.

EMSAs and DNA pulldown analyses, we observed that Sp1 and Sp3 bound to the GC-rich motif of *PROS1*, which was consistent with the findings of de Wolf *et al.* (38).

We did not observe the binding of ERα or interaction of ERα-Sp1 in the EMSAs; however, DNA pulldown assays showed that ERα bound to the *PROS1* promoter (−176/−147) in an E_2-dependent manner. This weak ERα binding seemed to depend on transfer from the cytoplasm to the nucleus by E_2 treatment. We also tried co-immunoprecipitation analyses but could not detect either the ERα-Sp1 or the ERα-Sp3 complex (data not shown). These observations were consistent with the report that a ternary ERα-Sp-DNA complex was not detected in gel mobility shift assays and that ERα enhances the formation of the Sp1-DNA complex and increases its stability (39). We hypothesized that ERα would bind to Sp-DNA complex *in vivo* feebly and that it could be too fragile to be detected as a supershifted band in EMSAs or in an ERα-Sp complex in co-immunoprecipitation analyses.

Through the RNA interference analysis, we found dual roles for Sp1 at the *PROS1* promoter in HepG2-ERα cells. Thus, knockdown of Sp1 or Sp3 resulted in substantially decreased transcriptional activity, indicating that both Sp1 and Sp3 take part in basal *PROS1* transcription as reported previously (38, 40). Intriguingly, we observed a loss of E_2-dependent *PROS1* repression in the cells transfected with iSp1, suggesting that Sp1 has a crucial role in the down-regulation of *PROS1* transcription by E_2. This highlights the potential dual function of Sp1 for basal activation and E_2-dependent repression of *PROS1* transcription.

Our study also showed that ERα might interact with Sp1 and repress *PROS1* expression via GC-rich motifs in its promoter region. GC-rich regions are known to be involved in ERα-mediated repression at the p21/WAF1 and cyclin G_2 gene promoters, where interplay with Sp proteins seems to occur (41, 42). Moreover, direct ER-Sp1 binding has been well documented in estrogen-stimulated genes (43). Actually, through chromatin immunoprecipitation assays, we showed that ERα and Sp1 bound to the responsive regions of the *PROS1* promoter simultaneously. Safe and Kim (39) stated previously that ERα enhances the formation of an Sp-DNA complex and increases its stability. Taken together, these findings suggested that Sp1 might retain its stability and bind more strongly to the regions of the *PROS1* promoter responsible to ERα.

Two pathways of E_2-ER signaling, a "classical" and a "non-classical" pathway, have been reported (25, 39). In the classical pathway, ligand-bound homodimeric ERs bind directly to a palindromic ERE or half-ERE in the promoter region of a target gene and modulate gene transcription by recruiting transcriptional coactivators or chromatin remodeling complexes. In the

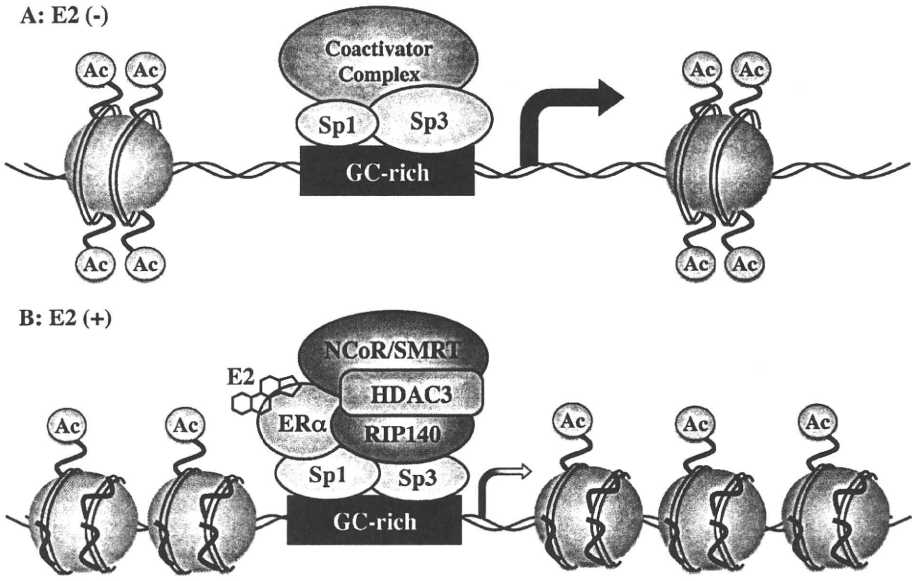

FIGURE 7. **A proposed model for down-regulation of *PROS1* promoter by 17β-estradiol in HepG2-ERα cells.** *A*, in HepG2-ERα cells without E_2 treatment, basal *PROS1* expression was regulated by Sp1 and Sp3, probably together with other transcriptional coactivators. *B*, in HepG2-ERα cells with E_2 treatment, *PROS1* expression was repressed by ERα-Sp1 interaction recruiting RIP140 and the NCoR-SMRT-HDAC3 corepressor complex sequentially, which consequently induced histone deacetylation. *Ac*, acetyl residue.

non-classical pathway, ligand-bound ERs do not bind to ERE directly; instead, they interact with other transcription factors such as Sp and AP-1 (39). ER-Sp or ER-AP-1 interaction mediates transcriptional gene regulation, recruiting cofactors or chromatin remodeling complexes to GC-rich motifs or to the AP-1 site in the target gene promoter. In this study, we have demonstrated that ERα-Sp1-RIP140 interaction regulates *PROS1* expression by recruiting the NCoR-SMRT corepressor complex and also HDAC3, which induces histone hypoacetylation and less permissive transcription of the *PROS1* gene.

An *in vivo* chromatin immunoprecipitation analysis of the E_2-responsive region in the *PROS1* promoter further revealed the recruitment of NCoR and SMRT to the *PROS1* modulator complex. NCoR and SMRT are now documented corepressors for nuclear receptors such as antagonist-bound estrogen receptors and progesterone receptors (44). It was reported that NCoR forms several different complexes with other transcription factors such as SMRT, Sin3a, and HDACs (44). In this study, we observed the recruitment of NCoR and SMRT corepressors to the *PROS1* promoter after E_2 treatment.

Liganded ERα, however, is not known to recruit NCoR-SMRT corepressors directly. Therefore, we tried ChIP assays for RIP140, which is known to interact with liganded ER and modulate ER-mediated transcription (35), and for LCoR, which is an NR-box-containing factor the same as RIP140 (36). We demonstrated that RIP140 was recruited to the target GC-rich region of the *PROS1* promoter after E_2 stimulation, but LCoR was not. The recruitment of RIP140 was theorized to correlate with the interaction between ERα and Sp1 because the effect of E_2 was destroyed by the knockdown of Sp1 in RNA interference analysis. We also found that the recruitment of NCoR-SMRT corepressors depended on ERα-Sp1 interaction and that the complex contained HDAC3. The NCoR-SMRT-HDAC3 interaction has been reported by several groups (45–48), consistent with our analysis of the *PROS1* promoter. The ChIP re-IP assays demonstrated that ERα-Sp1, RIP140, and NCoR-SMRT-HDAC3 were present in the same region of the *PROS1* promoter. Taken together with these data, this suggests that NCoR and SMRT were indirectly recruited as components of the HDAC3 complex by RIP140 through ERα-Sp1 interaction following E_2 stimulation.

Our proposed model for the down-regulation of *PROS1* expression by E_2 is depicted in Fig. 7. The repression of *PROS1* resembles the situation described for p21/WAF1 or cyclin G_2 (39, 49). In the absence of E_2, basal transcriptional regulation of *PROS1* seems to be mediated via multiple GC-rich regions including one at −172 to −153, as shown in this study and previously (38). In basal *PROS1* transcription, Sp1 and Sp3 are recruited to the promoter, and other transcription factors or coactivators may be involved. Upon E_2 treatment, ERα interacted and formed a complex with Sp1 at the GC-rich motifs of the *PROS1* promoter, and consequently ERα reinforced the stability of ERα-Sp1-DNA binding. Moreover, ERα-Sp1 interaction recruited RIP140, and consequently, RIP140 recruited the NCoR-SMRT-HDAC3 complex to the *PROS1* promoter. The NCoR-SMRT-HDAC3 complex might induce the hypoacetylation of histones, which could lead to greater stabilization of the nucleosome structure, limiting accessibility of the basal transcription factors and thus down-regulating *PROS1* expression.

To date, many genes have been reported to be stimulated by estrogen. Almost half of these estrogen-responsive genes may be repressed by estrogen (50); the mechanisms of estrogen-dependent repression have been elucidated. In this study, we have demonstrated novel mechanisms of E_2-induced *PROS1* repression, which could contribute to the elucidation of the estrogen action.

Meanwhile, our study has revealed that *PROS1* is a unique gene regulated both positively and negatively by Sp1 interaction in the same cell line. VEGFR2 is also regulated both positively and negatively by ERα-Sp protein interaction, but the type of regulation depends on the cell line, MCF7 or ZR-75 (51, 52). Interestingly, we reported previously a novel missense mutation at −168 from the ATG of the *PROS1* promoter (g.−168c>t), which results in weak promoter activity of *PROS1* (53). The mutation is located in the distal GC-rich motif, which could be critical for E_2-dependent repression, as shown in the current study. In addition, we obtained similar results in the EMSA using the oligo probe containing only distal GC-rich motif with or without mutation (data not shown). These data suggest that the distal GC-rich motif may be more important

than the proximal GC-rich motif. A patient carrying the g.−168c>t mutation showed decreased levels of plasma PS but supposedly did not show E_2-dependent *PROS1* repression (53).

In conclusion, we have demonstrated that *PROS1* expression is down-regulated by 17β-estradiol via ERα. ERα interacts with Sp1 and recruits RIP140. RIP140 associates directly with the HDAC3 complex containing NCoR-SMRT corepressors and induces the deacetylation of histones in the *PROS1* promoter. We have also revealed the dual roles of Sp1, which regulates *PROS1* expression both positively and negatively. E_2-dependent repression of *PROS1* results in reduced plasma PS levels, leading to the risk of deep venous thrombosis during pregnancy and oral contraceptive use. Further study will be required to fully characterize the mechanisms of reduction in PS and other possible mechanisms of regulation, such as using other hormones during pregnancy.

Acknowledgments—We greatly appreciate the pGL3 Basic-derived vector from Dr. Kokame (National Cardiovascular Center Research Institute, Suita, Japan). We also thank Drs. Akinobu Suzuki, Kanji Hirashima, Shinji Kunishima, Akira Katsmi, Koji Yamamoto, and Tadashi Matsushita for helpful discussions.

REFERENCES

1. Dahlbäck, B. (1991) *Thromb. Haemost.* **66,** 49–61
2. Heeb, M. J., Mesters, R. M., Tans, G., Rosing, J., and Griffin, J. H. (1993) *J. Biol. Chem.* **268,** 2872–2877
3. Heeb, M. J., Rosing, J., Bakker, H. M., Fernandez, J. A., Tans, G., and Griffin, J. H. (1994) *Proc. Natl. Acad. Sci. U.S.A.* **91,** 2728–2732
4. Schwarz, H. P., Fischer, M., Hopmeier, P., Batard, M. A., and Griffin, J. H. (1984) *Blood* **64,** 1297–1300
5. Engesser, L., Broekmans, A. W., Briët, E., Brommer, E. J., and Bertina, R. M. (1987) *Ann. Intern. Med.* **106,** 677–682
6. Makris, M., Leach, M., Beauchamp, N. J., Daly, M. E., Cooper, P. C., Hampton, K. K., Bayliss, P., Peake, I. R., Miller, G. J., and Preston, F. E. (2000) *Blood* **95,** 1935–1941
7. Gandrille, S., Borgel, D., Sala, N., Espinosa-Parrilla, Y., Simmonds, R., Rezende, S., Lind, B., Mannhalter, C., Pabinger, I., Reitsma, P. H., Formstone, C., Cooper, D. N., Saito, H., Suzuki, K., Bernardi, F., and Aiach, M. (2000) *Thromb. Haemost.* **84,** 918
8. D'Angelo, A., Vigano-D'Angelo, S., Esmon, C. T., and Comp, P. C. (1988) *J. Clin. Investig.* **81,** 1445–1454
9. Comp, P. C., Thurnau, G. R., Welsh, J., and Esmon, C. T. (1986) *Blood* **68,** 881–885
10. Malm, J., Laurell, M., and Dahlbäck, B. (1988) *Br. J. Haematol.* **68,** 437–443
11. Tans, G., Curvers, J., Middeldorp, S., Thomassen, M. C., Meijers, J. C., Prins, M. H., Bouma, B. N., Büller, H. R., and Rosing, J. (2000) *Thromb. Haemost.* **84,** 15–21
12. Fair, D. S., and Marlar, R. A. (1986) *Blood* **67,** 64–70
13. Fair, D. S., Marlar, R. A., and Levin, E. G. (1986) *Blood* **67,** 1168–1171
14. Ogura, M., Tanabe, N., Nishioka, J., Suzuki, K., and Saito, H. (1987) *Blood* **70,** 301–306
15. Maillard, C., Berruyer, M., Serre, C. M., Dechavanne, M., and Delmas, P. D. (1992) *Endocrinology* **130,** 1599–1604
16. Malm, J., He, X. H., Bjartell, A., Shen, L., Abrahamsson, P. A., and Dahlbäck, B. (1994) *Biochem. J.* **302,** 845–850
17. Benzakour, O., and Kanthou, C. (2000) *Blood* **95,** 2008–2014
18. Dahlbäck, B., and Stenflo, J. (1981) *Proc. Natl. Acad. Sci. U.S.A.* **78,** 2512–2516
19. Griffin, J. H., Gruber, A., and Fernández, J. A. (1992) *Blood* **79,** 3203–3211
20. Schmidel, D. K., Tatro, A. V., Phelps, L. G., Tomczak, J. A., and Long, G. L. (1990) *Biochemistry* **29,** 7845–7852
21. Ploos van Amstel, H. K., Reitsma, P. H., Van der Logt, C. P., and Bertina, R. M. (1990) *Biochemistry* **29,** 7853–7861
22. Edenbrandt, C. M., Lundwall, A., Wydro, R., and Stenflo, J. (1990) *Biochemistry* **29,** 7861–7868
23. de Wolf, C. J., Cupers, R. M., Bertina, R. M., and Vos, H. L. (2005) *J. Thromb. Haemost.* **3,** 410–412
24. Hall, J. M., Couse, J. F., and Korach, K. S. (2001) *J. Biol. Chem.* **276,** 36869–36872
25. Gruber, C. J., Tschugguel, W., Schneeberger, C., and Huber, J. C. (2002) *N. Engl. J. Med.* **346,** 340–352
26. Delfino, F., and Walker, W. H. (1999) *Mol. Cell. Endocrinol.* **157,** 1–9
27. Kushner, P. J., Agard, D. A., Greene, G. L., Scanlan, T. S., Shiau, A. K., Uht, R. M., and Webb, P. (2000) *J. Steroid Biochem. Mol. Biol.* **74,** 311–317
28. Levin, C. S. (2005) *Eur. J. Nucl. Med. Mol. Imaging* **32,** S325-S345
29. Safe, S., and Kim, K. (2004) *Prog. Nucleic Acid Res. Mol. Biol.* **77,** 1–36
30. Kokame, K., Kato, H., and Miyata, T. (2001) *J. Biol. Chem.* **276,** 9199–9205
31. Higuchi, R. (1990) in *PCR Protocols: A Guide to Methods and Applications* (Innis, M., Gelfand, D., Sninsky, J., and White, T., eds) pp. 177–183, Academic Press, San Diego
32. Sobue, S., Hagiwara, K., Banno, Y., Tamiya-Koizumi, K., Suzuki, M., Takagi, A., Kojima, T., Asano, H., Nozawa, Y., and Murate, T. (2005) *J. Neurochem.* **95,** 940–949
33. Furuhata, A., Murakami, M., Ito, H., Gao, S., Yoshida, K., Sobue, S., Kikuchi, R., Iwasaki, T., Takagi, A., Kojima, T., Suzuki, M., Abe, A., Naoe, T., and Murate, T. (2009) *Leukemia* **23,** 1270–1277
34. Suzuki, T., Fujisawa, J. I., Toita, M., and Yoshida, M. (1993) *Proc. Natl. Acad. Sci. U.S.A.* **90,** 610–614
35. Cavaillès, V., Dauvois, S., L'Horset, F., Lopez, G., Hoare, S., Kushner, P. J., and Parker, M. G. (1995) *EMBO J.* **14,** 3741–3751
36. White, J. H., Fernandes, I., Mader, S., and Yang, X. J. (2004) *Vitam. Horm.* **68,** 123–143
37. Wei, L. N., Hu, X., Chandra, D., Seto, E., and Farooqui, M. (2000) *J. Biol. Chem.* **275,** 40782–40787
38. de Wolf, C. J., Cupers, R. M., Bertina, R. M., and Vos, H. L. (2006) *J. Biol. Chem.* **281,** 17635–17643
39. Safe, S., and Kim, K. (2008) *J. Mol. Endocrinol.* **41,** 263–275
40. Tatewaki, H., Tsuda, H., Kanaji, T., Yokoyama, K., and Hamasaki, N. (2003) *Thromb. Haemost.* **90,** 1029–1039
41. Varshochi, R., Halim, F., Sunters, A., Alao, J. P., Madureira, P. A., Hart, S. M., Ali, S., Vigushin, D. M., Coombes, R. C., and Lam, E. W. F. (2005) *J. Biol. Chem.* **280,** 3185–3196
42. Stossi, F., Likhite, V. S., Katzenellenbogen, J. A., and Katzenellenbogen, B. S. (2006) *J. Biol. Chem.* **281,** 16272–16278
43. Porter, W., Saville, B., Hoivik, D., and Safe, S. (1997) *Mol. Endocrinol.* **11,** 1569–1580
44. Jepsen, K., and Rosenfeld, M. G. (2002) *J. Cell Sci.* **115,** 689–698
45. Jones, P. L., Sachs, L. M., Rouse, N., Wade, P. A., and Shi, Y. B. (2001) *J. Biol. Chem.* **276,** 8807–8811
46. Li, J., Wang, J., Wang, J., Nawaz, Z., Liu, J. M., Qin, J., and Wong, J. (2000) *EMBO J.* **19,** 4342–4350
47. Wen, Y. D., Perissi, V., Staszewski, L. M., Yang, W. M., Krones, A., Glass, C. K., Rosenfeld, M. G., and Seto, E. (2000) *Proc. Natl. Acad. Sci. U.S.A.* **97,** 7202–7207
48. Guenther, M. G., Lane, W. S., Fischle, W., Verdin, E., Lazar, M. A., and Shiekhattar, R. (2000) *Genes Dev.* **14,** 1048–1057
49. Owen, G. I., Richer, J. K., Tung, L., Takimoto, G., and Horwitz, K. B. (1998) *J. Biol. Chem.* **273,** 10696–10701
50. Frasor, J., Danes, J. M., Komm, B., Chang, K. C., Lyttle, C. R., and Katzenellenbogen, B. S. (2003) *Endocrinology* **144,** 4562–4574
51. Higgins, K. J., Liu, S., Abdelrahim, M., Yoon, K., Vanderlaag, K., Porter, W., Metz, R. P., and Safe, S. (2006) *Endocrinology* **147,** 3285–3295
52. Higgins, K. J., Liu, S., Abdelrahim, M., Vanderlaag, K., Liu, X., Porter, W., Metz, R., and Safe, S. (2008) *Mol. Endocrinol.* **22,** 388–402
53. Sanda, N., Fujimori, Y., Kashiwagi, T., Takagi, A., Murate, T., Mizutani, E., Matsushita, T., Naoe, T., and Kojima, T. (2007) *Br. J. Haematol.* **138,** 663–665

Thrombosis Research 125 (2010) e246–e250

Contents lists available at ScienceDirect

Thrombosis Research

journal homepage: www.elsevier.com/locate/thromres

Regular Article

A novel splice site mutation in intron C of *PROS1* leads to markedly reduced mutant mRNA level, absence of thrombin-sensitive region, and impaired secretion and cofactor activity of mutant protein S☆

Hiromi Okada [a,b,*], Shinji Kunishima [a], Motohiro Hamaguchi [a], Akira Takagi [c], Koji Yamamoto [d], Junki Takamatsu [d], Tadashi Matsushita [e], Hidehiko Saito [f], Tetsuhito Kojima [c], Tomio Yamazaki [a]

[a] Department of Hemostasis and Thrombosis, Clinical Research Center, National Hospital Organization Nagoya Medical Center, 4-1-1 San-nomaru, Naka-ku, Nagoya 460-0001, Japan
[b] Department of Educational Research Center for Clinical Pharmacy, Nagoya City University Graduate School of Pharmaceutical Sciences, Nagoya, Japan
[c] Department of Medical Technology, Nagoya University School of Health Sciences, Nagoya, Japan
[d] Department of Transfusion Medicine, Nagoya University Hospital, Nagoya, Japan
[e] Department of Hematology, Nagoya University Graduate School of Medicine, Nagoya Japan
[f] Nagoya Central Hospital, Nagoya, Japan

ARTICLE INFO

Article history:
Received 10 August 2009
Received in revised form 21 October 2009
Accepted 26 November 2009
Available online 21 December 2009

Keywords:
PROS1
protein S
splice site mutation
thrombosis
secretion
APC cofactor activity

ABSTRACT

Protein S (PS) is a member of the vitamin K-dependent protein family containing similar γ-carboxyglutamic acid (Gla) domains, although only PS has a thrombin-sensitive region (TSR), which is located between the Gla domain and the first epidermal growth factor-like domain. In this study, a novel *PROS1* mutation was identified at the last nucleotide in intron C (c.260-1G>A) in a patient suffering from recurrent deep vein thrombosis associated with PS deficiency. To investigate the molecular mechanisms of PS deficiency caused by the novel *PROS1* mutation, we characterized the mutant mRNA, and the secretion and function of the mutant PS molecule associated with the mutation. RT-PCR was used to detect the aberrant mRNA in the patient's platelets, the amount of which was markedly reduced and lacked the region corresponding to exon 4 coding the TSR of the PS molecule. The recombinant mutant PS lacking the TSR (TSR-lack PS) showed a markedly reduced transient expression/secretion level, 37.9% of that of wild-type (WT) PS. Activated protein C (APC) cofactor activity assay showed that TSR-lack PS had no cofactor activity. Moreover, binding assays of monoclonal antibodies recognizing the PS Gla domain and the Gla residues indicated that the bindings of TSR-lack PS to both of these antibodies were clearly weaker than those of WT PS. These findings suggest that the novel mutation leading to the absence of the TSR not only affected the secretion of mutant PS, but was also responsible for impairment of the Gla domain conformation required for the γ-carboxylation to express APC cofactor activity.

Introduction

Protein S (PS) is one of the most important natural anticoagulants, as demonstrated by the fact that individuals with PS deficiency have an increased risk of venous thrombosis [1]. PS enhances the activated protein C (APC)-dependent proteolytic inactivation of coagulation factor Va and factor VIIIa [2]. PS also exhibits APC-independent anticoagulant functions, probably through direct inhibition of both the prothrombinase and tenase complexes [3,4], and functions as a nonenzymatic cofactor for tissue factor pathway inhibitor in the inhibition of factor Xa [5–7]. Recently, model mice heterozygous for PS deficiency were generated and showed reduced PS plasma levels and APC cofactor activity in assays of plasma coagulation and thrombin generation [8]. It has also been reported that mice homozygous for PS deficiency were not obtained through mating and that the homozygous-recessive embryos died in utero, indicating the physiological importance of PS [8].

PS is a single-chain 635-amino-acid glycoprotein with a γ-carboxyglutamic acid (Gla) domain, a thrombin-sensitive region (TSR), four consecutive epidermal growth factor (EGF)-like domains, and a large domain homologous to the sex-hormone-binding

Abbreviations: PS, protein S; Gla, γ-carboxyglutamic acid; TSR, thrombin-sensitive region; WT, wild-type; APC, activated protein C; EGF, epidermal growth factor; DVT, deep vein thrombosis; ELISA, enzyme-linked immunosorbent assay; moAb, monoclonal antibody.

☆ A part of the data in this manuscript was presented at the 29th Congress of the Japanese Society on Thrombosis and Hemostasis, Utsunomiya, Japan, 18 November 2006, and the XXIst Congress of the International Society on Thrombosis and Haemostasis, Geneva, Switzerland, 9 July 2007.

* Corresponding author. Present address: Department of Educational Research Center for Clinical Pharmacy, Nagoya City University Graduate School of Pharmaceutical Sciences, 3-1 Tanabe-dori, Mizuho-ku, Nagoya 467-8603, Japan. Tel.: +81 52 836 3624; fax: +81 52 836 3621.
E-mail address: okada@phar.nagoya-cu.ac.jp (H. Okada).

0049-3848/$ – see front matter © 2009 Elsevier Ltd. All rights reserved.
doi:10.1016/j.thromres.2009.11.029

globulins. The Gla domain of PS is highly homologous to the Gla domains of other vitamin K-dependent coagulation factors and required to bind to the surface of negatively charged phospholipid membranes [9]. However, in contrast to other vitamin K-dependent factors, only PS has a unique module consisting of 29 residues, namely, the TSR, between the Gla domain and the EGF1 domain. The TSR is cleaved by thrombin at two sites (Arg-49 and Arg-70) and by factor Xa at Arg-60, resulting in functional inactivation of PS [10,11]. Although the physiological functions of the TSR are not yet fully understood, some studies have shown that the TSR is required for the PS Gla domain to bind to phospholipids [12]. These studies have also indicated that the TSR is not involved in direct interactions with phospholipids, but modulates phospholipid binding and the Gla domain conformation in a non-specific manner [13,14].

The PS gene, *PROS1* (GeneID: 5627), spans 101 kb of genomic DNA containing 15 exons and is transcribed into about 3.3 kb of mRNA. *PROS1* is located near the centromere of chromosome 3q11.1-11.2. To date, more than 200 mutations associated with PS deficiency in humans have been reported; however, only a few studies have investigated the molecular basis of the *PROS1* mutations responsible for PS deficiency. In the present study, we describe a novel splice site mutation in intron C of *PROS1* identified in a patient suffering from severe thrombotic complications associated with PS deficiency, and characterize the molecular effects of the mutation focusing on mutant mRNA levels, secretion of the mutant PS molecule, and the functional role of the TSR.

Materials and methods

Patient and blood samples

Patient

The patient is a Japanese man who had experienced episodes of recurrent deep vein thrombosis (DVT) in his legs since 45 years of age. Following pain in his left leg due to DVT at the age of 69, he was diagnosed with PS deficiency and has subsequently undergone continuous warfarin treatment. The PS levels in the patient's plasma showed total PS antigen, 30%; free PS antigen, 19%; and PS activity, < 10% under warfarin therapy.

Blood samples

This study was approved by the ethics committee of the Nagoya University School of Medicine. Following the provision of informed consent, venous blood samples from the patient with PS deficiency as well as normal individuals were collected. No blood samples were available from members of the patient's family. Genomic DNA and total platelet RNA containing PS mRNA were isolated as previously described [15].

Analysis of PS DNA and mRNA in platelets

PCR amplification and sequencing of *PROS1* and PS mRNA was done essentially as described previously elsewhere [15,16].

Mutagenesis and construction of expression vectors

The expression vector pcDNA3 (Invitrogen, San Diego, CA, USA) carrying a full-length WT PS cDNA was generously provided by Dr B. Dahlbäck. Mutant PS cDNA lacking exon 4 was generated by recombinant PCR [17]. The mutant PS molecule was designated as TSR-lack PS in this study.

Quantification of PS expression/secretion by ELISA and pulse-chase analysis

Transient expression of recombinant PS molecules in COS-1 cells and measurement of PS antigen concentration in conditioned media by an enzyme-linked immunosorbent assay (ELISA) were performed essentially following a previously described method [18,19]. Pulse-chase analysis of recombinant PS by radioactive labeling, immunoprecipitation, and electrophoresis were carried out as previously described [20].

Determination of APC cofactor activity of recombinant PS

In order to measure APC cofactor activity, we needed a large amount of recombinant PS. Thus, instead of transient transformants, we established stable transformants expressing recombinant PS molecules in HEK 293 cells as described previously [20]. The APC cofactor activity of recombinant PS was determined by a clotting-based assay as previously described [21].

Binding of the recombinant PS to monoclonal antibodies (moAbs)

Briefly, a microtiter plate was coated with two moAbs: moAb MK21 recognizing the PS Gla domain and moAb M3B recognizing the Gla residues (kindly provided by Dr B. Dahlbäck and Dr J. Stenflo, respectively) [22,23]. We also prepared a microtiter plate coated with anti-PS polyclonal antibody (DAKO, Glostrup, Denmark). For the binding assay, we prepared conditioned media containing recombinant PS molecules transiently expressed in COS-1 cells. Various concentrations of the recombinant PS were incubated in the coated plates with various antibodies overnight at 4 °C and bound proteins were detected by peroxidase-conjugated anti-PS polyclonal antibody (DAKO).

Results

Gene abnormalities in the patient

The DNA-PCR products of all 15 exons, including exon-intron boundaries, of *PROS1* in the patient were directly sequenced. A G-to-A substitution at the last nucleotide of intron C was identified in exon 4 of the DNA-PCR products. This novel mutation (c.260-1G>A) was found to be heterozygous in the patient. The same mutation was not found in the DNA samples of 114 healthy subjects (data not shown).

The total platelet RNA in the patient was tested for the presence of mutant PS mRNA. Using the primers shown in the legend to Fig. 1, the region including exon 4 was amplified by RT-PCR. An aberrant, small RT-PCR product was detected in addition to a band associated with the normal-sized product (404 bp) for the patient, but not for the controls (Fig. 1). Furthermore, the abnormal band showed a significantly lower intensity compared with the normal band. Each product was purified by gel electrophoresis and directly sequenced. The normal sized product showed only the WT sequence of *PROS1*; however, the sequence of the aberrant fragment completely lacked exon 4 (c.260_346del: p.Val87_Asn115del).

The expression/secretion of recombinant PS in COS-1 cells

The failure to transcribe exon 4 causes an in-frame deletion of 29 amino acids that constitute the TSR of the PS molecule. To address the effect of the absence of TSR in the mutant PS on its expression/secretion from cells, transient expression studies with COS-1 cells were performed and the culture media were analyzed for recombinant PS content. To accurately quantify these recombinant PS expression/secretion levels, the concentrations of recombinant PS in the culture media were measured by ELISA (Fig. 2A). The quantity of TSR-lack PS in the culture media was markedly reduced to 37.9% of that of WT PS.

Pulse-chase analysis was carried out to compare the secretion profile of TSR-lack PS with that of WT PS (Fig. 2B). The level of radiolabeled WT PS rapidly decreased in the cells with a half-life of 2

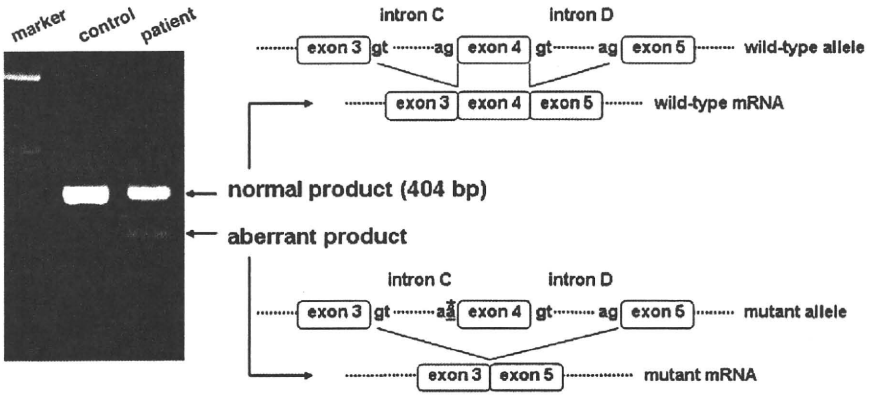

Fig. 1. Analysis of the PS mRNA of the patient with PS deficiency. Left: RT-PCR products amplified with the primer set (5′-AGGCTTCACAAGTCCTGGTTAGGAAGCG-3′ and 5′-CTTTGATTTGAGATTATATCTGTAGCC-3′) were subjected to electrophoresis on a 2% agarose gel and stained with ethidium bromide. Right: Schematic diagram indicates the mechanism causing the absence of exon 4 in the aberrant RT-PCR product of the patient induced by the G-to-A transition (*) at the splice site at -1 of exon 4 (c.260-1G>A). Raw sequencing data of the normal RT-PCR product and the aberrant RT-PCR product are not shown.

hours and immediately appeared in the culture media. In contrast, radiolabeled TSR-lack PS slowly disappeared from the cells, with a half-life of approximately 8 hours, and its rate of secretion into the culture media was lower than that of WT PS. Furthermore, the secretion efficiency, measured as the level of PS in the media at 8 hours, was significantly reduced for TSR-lack PS (40% of the initial value) compared with WT PS (70%). Taken together, these findings show not only that the secretion rate of TSR-lack PS is lower than that of WT PS, but also that the secretion efficiency of TSR-lack PS is lower.

APC cofactor activity

The APC cofactor activities of WT PS and TSR-lack PS were examined by a clotting-based assay using the serum-free culture media of the stable transformants. WT PS dose-dependently prolonged the clotting time (10-100 ng/ml), while TSR-lack PS showed no APC cofactor activity (Fig. 3).

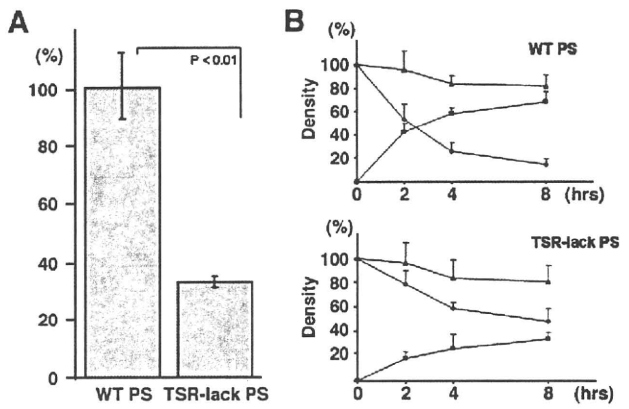

Fig. 2. Transient expression/secretion of WT PS and TSR-lack PS in COS-1 cells. (A) ELISA results of concentration of WT PS and TSR-lack PS. Mean value of WT PS is assigned as 100%. Values represent mean ± SD of 6 transfection experiments for both WT PS and TSR-lack PS. Comparison between TSR-lack PS and WT PS expression levels was performed using unpaired *t*-test. (B) Pulse-chase analysis using transient expression in COS-1 cells. Radiolabeled media and cell lysates were immunoprecipitated and subjected to SDS-PAGE. The radioactivity of the PS bands on the dried gels was measured using an image analyzer. The amount of radioactive PS in the cell lysates at the beginning of the experiment is assigned a value of 100%. Graphs represent radioactivity recovered from cell lysates (♦), media (■), or the total (▲) at each time point. Total radioactivity was calculated as the sum of radioactivities recovered from media and lysates. Values represent mean ± SD of 3 (WT PS) or 4 (TSR-lack PS) independent experiments.

Binding of recombinant PS to moAbs recognizing the PS Gla domain and the Gla residues

Next, to identify the effect of the absence of the TSR in the PS molecule on its Gla domain conformation and γ-carboxylation, we performed moAbs binding assays using the serum-free culture media of transient transformants (Fig. 4). WT PS and TSR-lack PS showed similar binding to the anti-PS polyclonal antibody. In contrast, in the Ca^{2+}-dependent and conformation-dependent moAb MK21 (recognizing the PS Gla domain) binding assay, the binding of TSR-lack PS was weaker than that of WT PS, as described in previous reports [14]. In addition, the binding of TSR-lack PS to the moAb M3B (recognizing the Gla residues) was also clearly weaker than that of WT PS, suggesting that TSR-lack PS has impaired γ-carboxylation.

Discussion

In the present study, the DNA analysis of a patient with PS deficiency revealed a G-to-A transition at the last nucleotide of intron C of *PROS1* (c.260-1G>A). This novel point mutation abolishes the invariant AG dinucleotide in the acceptor splice site of intron C and

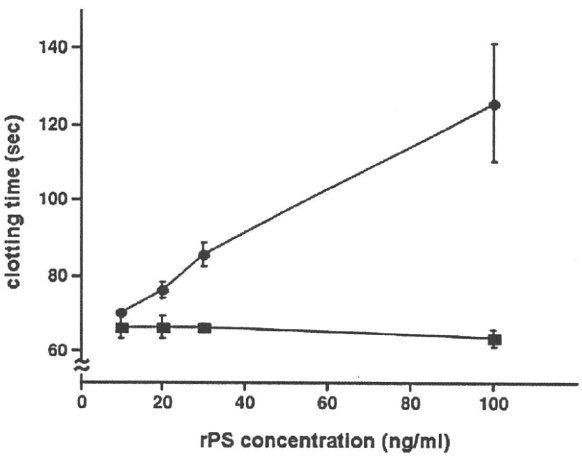

Fig. 3. APC cofactor activity of WT PS and TSR-lack PS. WT PS and TSR-lack PS at a range of concentrations (0-100 ng/mL) in serum-free media of stable transformants were incubated with PS-depleted plasma, factor Va, and APC for 2 min. Clotting was initiated by addition of $CaCl_2$, and clotting time was measured using ST art4. Values represent mean ± SD of 6 independent experiments. (●) indicates WT PS; (■), TSR-lack PS.

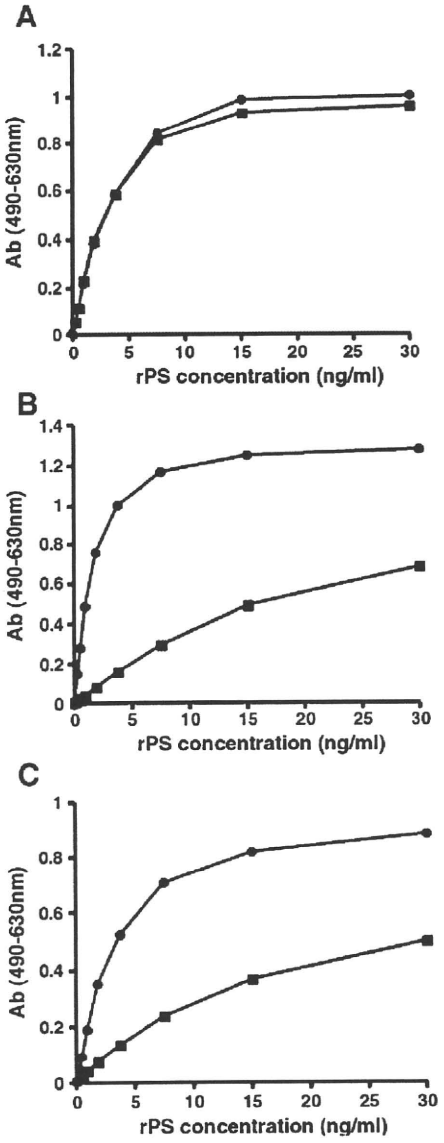

Fig. 4. Characterization of the Gla domain conformation and the γ-carboxylation of recombinant PS. The binding of WT PS (●), and TSR-lack PS (■) to polyclonal anti-PS antibody (A), moAb MK21 recognizing the PS Gla domain that is Ca^{2+}- and conformation-dependent (B), and the moAb M3B recognizing the Gla residues (C) in the culture media were measured by microtiter plate assay. The bound recombinant PS molecules were detected using peroxidase-conjugated anti-PS polyclonal antibody.

may subsequently induce cryptic splicing of the mutated mRNA [24]. Okamoto et al. reported that the region corresponding to exon 4 of *PROS1* containing a nonsense mutation (c.308C>G: p.Ser103X) was absent in mutant mRNA, and that the amount of the abnormal PS transcript was markedly reduced in a patient with a quantitative PS deficiency [25]. In fact, our RT-PCR analysis also revealed the presence of aberrant mRNA lacking a section corresponding to exon 4, the amount of which was markedly reduced in our patient. It was supposed that this splice site mutation affected the splicing of the aberrant pre-mRNA and impaired the mRNA processing efficiency, and possibly also the *in vivo* stability of the aberrant mRNA which could be lower than that of WT mRNA, resulting in the low mutant mRNA level [26]. It is apparent that the reduced mRNA level associated with the failed transcription of an exon caused by the splice site mutation is mainly responsible for the quantitative PS deficiency in our patient.

The failed transcription of exon 4 causes an in-frame deletion of 29 amino acids that constitute the TSR of the PS molecule (c.260_346del: p.Val87_Asn115del). The complete deletion of a domain as important as the TSR is expected to affect protein structure and function. To demonstrate the effect of the absence of the TSR in the PS molecule on its expression/secretion from cells, we carried out transient expression analysis using COS-1 cells. Measurement of the amount of protein secreted into the culture media by ELISA is useful for assessing the overall efficiency of the protein expression/secretion pathway because an ELISA result depends on the efficiency of every step of the expression/secretion pathway, including transcription, mRNA stability, translation, secretion, and protein stability in the culture medium. In addition, we performed pulse-chase analysis to focus on the steps from primary protein synthesis to secretion in the protein expression/secretion pathway. Our ELISA result showed that the amount of TSR-lack PS secreted into the culture medium was markedly reduced to 37.9% of that of WT PS, indicating that some steps in the protein expression/secretion pathway were impaired. Moreover, the data from pulse-chase analysis also showed that the secretion efficiency of TSR-lack PS was significantly lower than that of WT PS. Thus, it is considered that the absence of the TSR in the PS molecule leads to its impaired secretion, resulting in the quantitative PS deficiency similar to the missense mutations associated with quantitative PS deficiency reported previously [27]. The present study indicates that not only the decrease in the level of mutant mRNA, but also the impairment of mutant PS secretion, is responsible for the quantitative PS deficiency in the patient.

In some reports, the TSR of PS is described as being essential for APC cofactor activity, because the TSR is necessary to maintain the correct conformation of the PS Gla domain for its binding to membranes [12,13]. Our data clearly show that TSR-lack PS has no APC cofactor activity, in contrast to WT PS, in the clotting-based assay (Fig. 3). In addition, the binding assay of moAb MK21 recognizing the PS Gla domain showed that TSR-lack PS bound to MK21 with significantly lower affinity than WT PS, indicating that the Gla domain might be incorrectly folded in TSR-lack PS (Fig. 4B). Furie et al reported that the vitamin K-dependent proteins lack biological activity if γ-carboxylation is impaired [28]. We also demonstrated that the binding affinity of TSR-lack PS to the moAb M3B, which recognizes the Gla residues, was much lower than that of WT PS (Fig. 4C), indicating that the γ-carboxylation of TSR-lack PS was at least partially impaired. Therefore, it was speculated that the absence of the TSR affected the conformation of the γ-carboxylase-recognizing region near the Gla domain of the PS molecule, leading to partial impairment of the γ-carboxylation of TSR-lack PS. Our findings suggest that the TSR of PS might have an important role in maintaining the conformation of the Gla domain of PS required for its proper γ-carboxylation, and that the absence of the TSR might result in the loss of APC cofactor activity.

Unfortunately, we were unable to measure the levels of plasma PS before the patient started warfarin therapy, which makes it difficult to discuss the genotype-phenotype relationship in detail. However, our observations suggest that in our patient, the plasma antigen concentration of TSR-lack PS is very low because of the reduced mutant mRNA level and the impaired secretion of TSR-lack PS. Furthermore, even though a small amount of TSR-lack PS was identified in the plasma, it is expected to be inactive as an APC cofactor. Thus, we consider that the patient would have low plasma PS antigen and activity levels even if he had not undergone the warfarin treatment. In this study, we identified a novel splice site mutation in *PROS1* leading to a reduced mutant mRNA level and the absence of the TSR in the mutant PS molecule. We also characterized the mutant TSR-lack PS molecule to investigate the molecular effects of the mutation. These molecular approaches could contribute to a greater understanding of the relationship between the genetic mutation and clinical phenotypes.

Conflict of interest statement

The authors declare that they do not have conflict of interest with respect to this manuscript.

Acknowledgements

We wish to thank C. Wakamatsu for her expert technical assistance. This study was supported in part by Grants-in-Aid from the Japanese Ministry of Education, Culture, Sports, Science and Technology (17590490) and the Japanese Ministry of Health, Labor and Welfare (Research on Measures for Intractable Diseases).

References

[1] Makris M, Leach M, Beauchamp NJ, Daly ME, Cooper PC, Hampton KK, Bayliss P, Peake IR, Miller GJ, Preston FE. Genetic analysis, phenotypic diagnosis, and risk of venous thrombosis in families with inherited deficiencies of protein S. Blood 2000;95:1935–41.
[2] Dahlbäck B. Protein S and C4b-binding protein: components involved in the regulation of the protein C anticoagulant system. Thromb Haemost 1991;66:49–61.
[3] Hackeng TM, van 't Veer C, Meijers JC, Bouma BN. Human protein S inhibits prothrombinase complex activity on endothelial cells and platelets via direct interactions with factors Va and Xa. J Biol Chem 1994;269:21051–8.
[4] Koppelman SJ, Hackeng TM, Sixma JJ, Bouma BN. Inhibition of the intrinsic factor X activating complex by protein S: evidence for a specific binding of protein S to factor VIII. Blood 1995;86:1062–71.
[5] Hackeng TM, Sere KM, Tans G, Rosing J. Protein S stimulates inhibition of the tissue factor pathway by tissue factor pathway inhibitor. Proc Natl Acad Sci USA 2006;103:3106–11.
[6] Rosing J, Maurissen LF Tchaikovski SN, Tans G, Hackeng TM. Protein S is a cofactor for tissue factor pathway inhibitor. Thromb Res 2008(SV):60–3.
[7] Ndonwi M, Broze Jr G. Protein S enhances the tissue factor pathway inhibitor inhibition of factor Xa but not its inhibition of factor VIIa-tissue factor. J Thromb Haemost 2008;6:1044–6.
[8] Saller F, Brisset AC, Tchaikovski SN, Azevedo M, Chrast R, Fernandez JA, Schapira M, Hackeng TM, Griffin JH and Angelillo-Scherrer A. Generation and phenotypic analysis of protein S-deficient mice. Blood. In Press 2009.
[9] Walker FJ. Regulation of activated protein C by protein S. The role of phospholipid in factor Va inactivation. J Biol Chem 1981;256:11128–31.
[10] Lu D, Xie RL, Rydzewski A, Long GL. The effect of N-linked glycosylation on molecular weight, thrombin cleavage, and functional activity of human protein S. Thromb Haemost 1997;77:1156–63.
[11] Long GL, Lu D, Xie RL, Kalafatis M. Human protein S cleavage and inactivation by coagulation factor Xa. J Biol Chem 1998;273:11521–6.
[12] Borgel D, Gaussem P, Garbay C, Bachelot-Loza C, Kaabache T, Liu WQ, Brohard-Bohn B, Le Bonniec B, Aiach M, Gandrille S. Implication of protein S thrombin-sensitive region with membrane binding via conformational changes in the gamma-carboxyglutamic acid-rich domain. Biochem J 2001;360:499–506.
[13] Saller F, Villoutreix BO, Amelot A, Kaabache T, Le Bonniec BF, Aiach M, Gandrille S, Borgel D. The gamma-carboxyglutamic acid domain of anticoagulant protein S is involved in activated protein C cofactor activity, independently of phospholipid binding. Blood 2005;105:122–30.
[14] Saller F, Kaabache T, Aiach M, Gandrille S, Borgel D. The protein S thrombin-sensitive region modulates phospholipid binding and the gamma-carboxyglutamic acid-rich (Gla) domain conformation in a non-specific manner. J Thromb Haemost 2006;4:704–6.
[15] Yamazaki T, Hamaguchi M, Katsumi A, Kagami K, Kojima T, Takamatsu J, Saito H. A quantitative protein S deficiency associated with a novel nonsense mutation and markedly reduced levels of mutated mRNA. Thromb Haemost 1995;74:590–5.
[16] Iwaki T, Mastushita T, Kobayashi T, Yamamoto Y, Nomura Y, Kagami K, Nakayama T, Sugiura I, Kojima T, Takamatsu J, Kanayama N, Saito H. DNA sequence analysis of protein S deficiency identification of four point mutations in twelve Japanese subjects. Semin Thromb Hemost 2001;27:155–60.
[17] Higuchi R. Recombinant PCR. In: innis MA, Gelfand DH, Sninsky JJ, White TJ, editors. PCR Protocols. San Diego, CA: Academic Press; 1990. p. 177–83.
[18] Whitt M, Buonocore L, Rose JK. Liposome-mediated transfection. Curr Protoc Immunol 2001 Chapter 10:Unit 10 6.
[19] Espinosa-Parrilla Y, Yamazaki T, Sala N, Dahlbäck B, Garcia de Frutos P. Protein S secretion differences of missense mutants account for phenotypic heterogeneity. Blood 2000;95:173–9.
[20] Giri TK, Garcia de Frutos P, Yamazaki T, Villoutreix BO, Dahlbäck B. In vitro characterisation of two naturally occurring mutations in the thrombin-sensitive region of anticoagulant protein S. Thromb Haemost 1999;82:1627–33.
[21] Okada H, Yamazaki T, Takagi A, Murate T, Yamamoto K, Takamatsu J, Matsushita T, Naoe T, Kunishima S, Hamaguchi M, Saito H, Kojima T. In vitro characterization of missense mutations associated with quantitative protein S deficiency. J Thromb Haemost 2006;4:2003–9.
[22] Brown MA, Stenberg LM, Persson U, Stenflo J. Identification and purification of vitamin K-dependent proteins and peptides with monoclonal antibodies specific for gamma -carboxyglutamyl (Gla) residues. J Biol Chem 2000;275:19795–802.
[23] Dahlbäck B, Hildebrand B, Malm J. Characterization of functionally important domains in human vitamin K-dependent protein S using monoclonal antibodies. J Biol Chem 1990;265:8127–35.
[24] Cooper DN. Human gene mutations affecting RNA processing and translation. Ann Med 1993;25:11–7.
[25] Okamoto Y, Yamazaki T, Katsumi A, Kojima T, Takamatsu J, Nishida M, Saito H. A novel nonsense mutation associated with an exon skipping in a patient with hereditary protein S deficiency type I. Thromb Haemost 1996;75:877–82.
[26] Wang GS, Cooper TA. Splicing in disease: disruption of the splicing code and the decoding machinery. Nature Rev Genet 2007;8:749–61.
[27] Okada H, Takagi A, Murate T, Adachi T, Yamamoto K, Matsushita T, Takamatsu J, Sugita K, Sugimoto M, Yoshioka A, Yamazaki T, Saito H, Kojima T. Identification of protein S alpha gene mutations including four novel mutations in eight unrelated patients with protein S deficiency. Br J Haematol 2004;126:219–25.
[28] Furie B, Bouchard BA, Furie BC. Vitamin K-dependent biosynthesis of gamma-carboxyglutamic acid. Blood 1999;93:1798–808.

Int J Hematol (2010) 92:405–408
DOI 10.1007/s12185-010-0659-9

LETTER TO THE EDITOR

Severe hemophilia A in a Japanese female caused by an *F8*-intron 22 inversion associated with skewed X chromosome inactivation

Yuhri Miyawaki · Atsuo Suzuki · Yuhta Fujimori · Akira Takagi · Takashi Murate · Nobuaki Suzuki · Akira Katsumi · Tomoki Naoe · Koji Yamamoto · Tadashi Matsushita · Junki Takamatsu · Tetsuhito Kojima

Received: 19 May 2010 / Revised: 12 July 2010 / Accepted: 28 July 2010 / Published online: 11 August 2010

Hemophilia A is an X-linked recessive bleeding disorder with a worldwide prevalence of approximately 1 in 5,000 males. Hemophilia A is caused by a deficiency or functional defect in coagulation factor VIII (FVIII), and its clinical severity is inversely related to residual FVIII activity (FVIII:C). Patients with less than 1, 1–5, and 5–30% FVIII:C are classified as having severe, moderate, and mild hemophilia A, respectively [1]. The gene encoding FVIII (*F8*) is located in the most distal region of the long arm of the X chromosome (Xq28) and spans 186 kb [2]. The molecular basis underlying hemophilia A is well characterized, and various causative defects, such as point mutations, insertions, deletions and other genetic abnormalities, have been found in the *F8* gene of hemophilia A patients. Among them, a large genomic inversion disrupting *F8* at intron 22 (*F8-int22* inversion) is found in about half of severe hemophilia A cases including Japanese [3–5], and an inversion at intron 1 (*F8-int1* inversion) is found in 1–5% of cases [6, 7].

Hemophilia A affects males, and is transmitted by heterozygous females who are denoted as carriers. They are usually asymptomatic, because their proportion of somatic cells with an inactivated normal X chromosome is approximately equal to the proportion with an inactivated mutated X chromosome [8]. However, there are several potential genetic mechanisms leading to the phenotypic expression of very low FVIII:C in female carriers as hemophiliacs. Thus, in rare cases, severe hemophilia A can occur in females homozygous (e.g., consanguinity) or compound heterozygous for mutations in *F8* [9, 10], through X chromosome abnormalities such as monosomy X (45 X, Turner syndrome), and due to skewed X inactivation in a heterozygous female carrier [11, 12]. In this study, we investigated the genetic mechanisms of *F8* defects to elucidate the molecular pathogenesis responsible for severe hemophilia A in a Japanese female. The study was approved by the Ethics Committee of the Nagoya University School of Medicine, and genomic DNA samples from all participants were isolated from peripheral leukocytes by phenol extraction as described previously [13], after informed consents were obtained.

The patient was a 21-year-old female and suffered from bleeding symptoms, such as easy bruising and joint swelling, since she was 2 years old. She was diagnosed as a severe hemophilia A (FVIII:C < 1% and FVIII:Ag < 5%), and received FVIII concentrates as replacement therapy. However, she had developed hemophiliac arthropathy in her left elbow joint. Her elder brother suffered from similar bleeding symptoms and had also been diagnosed as a severe hemophilia A (FVIII:C < 1% and FVIII:Ag < 5%).

Y. Miyawaki · A. Suzuki · Y. Fujimori · A. Takagi · T. Murate · T. Kojima
Department of Pathophysiological Laboratory Sciences, Nagoya University Graduate School of Medicine, Nagoya, Japan

A. Takagi · T. Murate · T. Kojima (✉)
Department of Medical Technology, Nagoya University School of Health Sciences, 1-1-20 Daiko-Minami, Higashi-ku, Nagoya 461-8673, Japan
e-mail: kojima@met.nagoya-u.ac.jp

N. Suzuki · A. Katsumi · T. Naoe
Department of Hematology-Oncology, Nagoya University Graduate School of Medicine, Nagoya, Japan

K. Yamamoto · T. Matsushita
Division of Transfusion Medicine, Nagoya University Hospital, Nagoya, Japan

J. Takamatsu
Aichi Red Cross Blood Center, Seto, Japan

The mother was a hemophiliac carrier (FVIII:C = 48% and FVIII:Ag = 61%). The levels of von Willebrand factor antigen and ristocetin cofactor activity in all family members tested including the patients were within the normal range. A DNA sample from the father was not available. Chromosomal analysis of the patient revealed a normal female 46, XX karyotype with no structural abnormalities (data not shown).

The pedigree of the patient's family is shown in Fig. 1. First, we analyzed inversions of *F8-int22* and *F8-int1* by the inverse shifting-polymerase chain reaction (IS-PCR) approach [14], and found that the patient was heterozygous for *F8-int22* inversion type I mutation (data not shown). We detected the same *F8-int22* inversion in her brother monozygously and in her mother heterozygously. These results indicated the *F8-int22* inversion found in the patient to be inherited from her mother. We also tested for the *F8-int22* inversion in their DNA by Southern blotting [15] as well as by single-tube long-distance PCR (LD-PCR) [6, 16], and obtained consistent results with the IS-PCR data (data not shown).

Female carriers with a heterozygous abnormal *F8* gene show generally about 50% of FVIII:C due to random inactivation of the X chromosomes with a rate equivalence. The patient was diagnosed as a hemophilia A carrier with the *F8-int22* inversion in terms of genotype, but with a severe hemophilia A phenotype. Because the skewed X chromosome inactivation in a heterozygous carrier is known to be a cause of X-linked recessive disorders in females [8], we

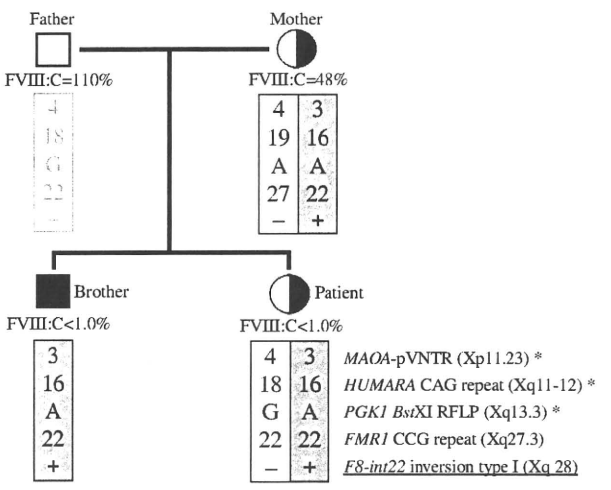

Fig. 1 Pedigree and X chromosome haplotypes of the family members. FVIII:C levels (%) were represented *below the symbols*. Haplotypes of the X chromosomes were shown in *boxes*, and represented the number of repeats, individual nucleotides, or presence/absence (+/−) of the mutation at each locus. A predicted haplotype of the father, for whom data were unavailable, was shown in *bright gray*. *Informative markers for the assessment of the X chromosome inactivation pattern of the patient

tried to examine the DNA methylation pattern at the heterozygous X-linked gene loci. First, we determined the chromosome haplotype of the family members, and found that three markers, the monoamine oxidase A gene (*MAOA*, Xp11.23) promoter VNTR (*MAOA*-pVNTR) [17], the human androgen receptor gene (*HUMARA*, Xq11–12) CAG repeat [18] and the phosphoglycerate kinase 1 gene (*PGK1*, Xq13.3) *Bst*XI polymorphism [19], were informative, but the fragile X mental retardation gene 1 (*FMR1*, Xq27.3) CGG repeat [20] was not (Fig. 1).

Among them, we assessed the DNA methylation pattern at *MAOA*-pVNTR as shown in Fig. 2. Since *Hpa*II cleaves non-methylated DNA in the active X chromosome, PCR amplification of the gene in DNA treated with *Hpa*II will fail. In the sample of the patient's brother having a single active X chromosome, PCR-amplified fragments appeared as a 210-bp band (3-repeats allele, lane 5), but disappeared on digestion of the template DNA with *Hpa*II (lane 6). The analysis of PCR-amplified fragments from the mother's DNA samples with or without digestion by *Hpa*II showed two distinct bands, a 4-repeats allele (240-bp) and a 3-repeats allele (210-bp) (lanes 3 and 4), suggesting that random X inactivation occurred in her somatic cells. In contrast, the DNA of the patient not digested with *Hpa*II gave two distinct bands (lane 1), a 4-repeats allele from the father (240-bp) and a 3-repeats allele from the mother (210-bp), but only the 240-bp band was observed on PCR amplification of the *Hpa*II-digested DNA sample (lane 2). Analysis of this pattern with NIH image version 1.62 revealed an extremely skewed inactivation of the paternally derived X chromosome containing a normal *F8* (ratio 99.5: 0.5), fully consistent with the patient's severe hemophilia A phenotype. We also analyzed X chromosome inactivation patterns at the other two gene markers, the *HUMARA* CAG repeat and the *PGK1 Bst*XI polymorphism, and obtained similar findings with skewed inactivation rates (data not shown). Meanwhile, we analyzed the *F8* genomic sequence of the patient by PCR-mediated direct sequencing, and found no abnormality causing a FVIII deficiency (data not shown). Taken together, it was suggested that an extremely skewed inactivation toward the paternally derived X chromosome carrying a normal *F8* gene could occur in this female hemophilia A patient.

X chromosome inactivation is a process in mammals by which one of the two X chromosomes in female somatic cells is inactivated to eliminate differences between males and females in levels of expression of the genes on the X chromosome [21]. The determination of whether the maternally or paternally derived X chromosome is to be inactivated is random, and the inactive X chromosome is silenced by CpG hyper-methylation. X chromosome inactivation is regulated by the expression of the X-inactive-specific transcript gene (*XIST*) [22]. The *XIST* antisense

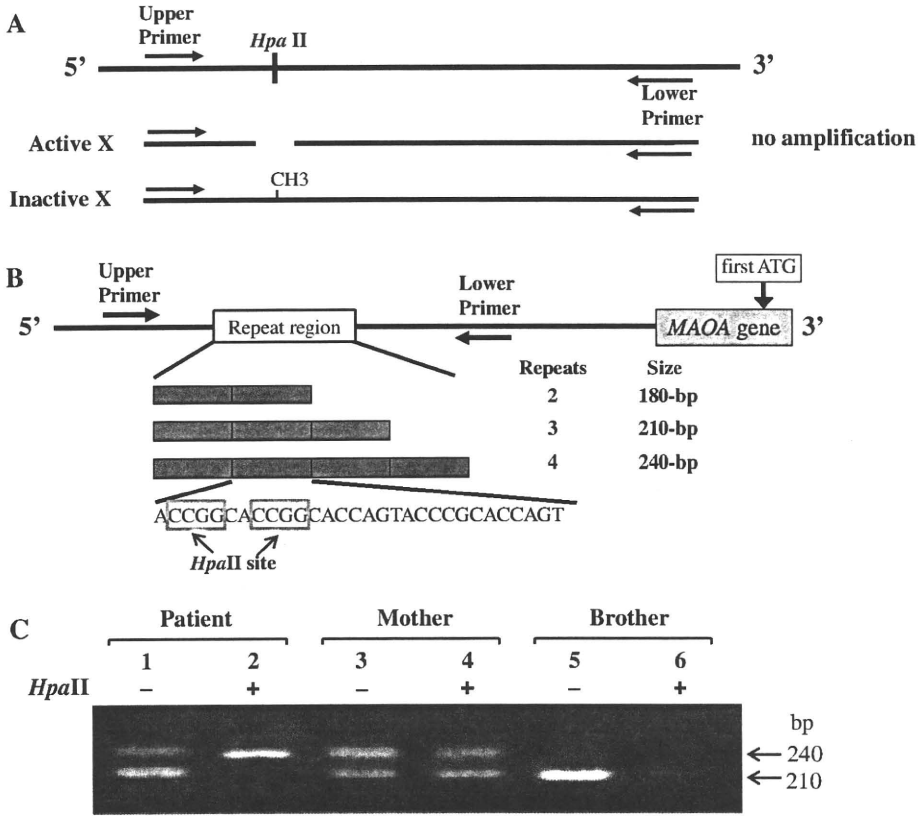

Fig. 2 Assessment of X chromosome inactivation at *MAOA*-pVNTR. **a** Scheme of methylation-sensitive *Hpa*II-PCR amplification at *MAOA*-pVNTR. The symbol (^{CH3}) indicated a methylation site in the *Hpa*II cleavage site of the gene. Since *Hpa*II cleaves non-methylated DNA in the active X chromosome, PCR amplification of the *Hpa*II-treated gene on the active X chromosome will fail. **b** Scheme of the *MAOA* gene and *MAOA*-pVNTR repeat sequence. Repeat structure, sequence of the repeat region, allele (repeat) numbers, and PCR product sizes were shown. *Solid arrows* indicate a PCR primer set. **c** Methylation-sensitive *Hpa*II-PCR patterns at *MAOA*-pVNTR. After digestion of the DNA with *Hpa*II, PCR-mediated *MAOA*-pVNTR for the patient showed an extremely unbalanced amplification toward the paternal 4-repeats allele. Comparatively, that for the mother showed nearly equal levels of amplification for both alleles. +: *Hpa*II-predigested DNA, −: undigested DNA

RNA (*TSIX*), which is an RNA gene and a negative regulator of *XIST*, is also related to this process [23]. A skewed X chromosome can occur as a result of chance, abnormalities in these factors, or selection that eliminates the normal X chromosome after X inactivation [8]. We did not elucidate the precise mechanisms responsible for the skewed X inactivation in this patient; however, it might be possible due to an aberration of these factors.

In conclusion, the maternally transmitted *F8-int22* inversion and the extremely skewed inactivation of the paternally derived X chromosome carrying a normal *F8* would cause the severe hemophilia A phenotype in this female patient, although the presence of other mutation cannot be excluded completely.

Acknowledgments The authors thank C. Wakamatsu for her expert technical assistance, and the members of the Kojima laboratory and Dr. H. Saito for helpful discussions. This study was supported in part by Grants-in-Aid from the Kitamura Memorial Foundation, the Baxter Hemophilia Scientific Research & Education Fund (BHF) and the Japanese Ministry of Health, Labour and Welfare (Research on Measures for Intractable Diseases).

References

1. White GC II, Rosendaal F, Aledort LM, Lusher JM, Rothschild C, Ingerslev J, et al. Definitions in hemophilia. Recommendation of the scientific subcommittee on factor VIII and factor IX of the scientific and standardization committee of the International Society on Thrombosis and Haemostasis. Thromb Haemost. 2001;85:560.
2. Gitschier J, Wood WI, Goralka TM, Wion KL, Chen EY, Eaton DH, et al. Characterization of the human factor VIII gene. Nature. 1984;312:326–30.
3. Lakich D, Kazazian HH, Antonarakis SE, Gitschier J. Inversions disrupting the factor VIII gene are a common cause of severe haemophilia A. Nat Genet. 1993;5:236–41.
4. Naylor J, Brinke A, Hassock S, Green PM, Giannelli F. Characteristic mRNA abnormality found in half the patients with